University of Helsinki

Faculty of Science

Department of Chemistry

Funded by the Erasmus+ Programme of the European Union

Erasmus Mundus Joint Master Degree

"Advanced Spectroscopy in Chemistry"

MASTER THESIS

by

Narmin Suvarli

July, 2018

Helsinki, Finland

Manipulating Thermoresponsive Properties of Polycations in Water

Laboratory: Polymers and Colloids

Supervisor: Prof. Heikki Tenhu, Dr. Erno Karjalainen

Reviewers: Prof. Sirkka Liisa Maunu, Ph. D. Erno Karjalainen

HELSINGIN YLIOPISTO
HELSINGFORS UNIVERSITET
UNIVERSITY OF HELSINKI

MATEMAATTIS-LUONNONTIETEELLINEN TIEDEKUNTA
MATEMATISK-NATURVETENSKAPLIGA FAKULTETEN
FACULTY OF SCIENCE

Tiedekunta – Fakultet – Faculty	Koulutusohjelma – Utbildningsprogram – Degree programme	
Faculty of Science	***Master's Programme in Chemistry and Molecular Sciences - ASC***	
Tekijä – Författare – Author ***Narmin Suvarli***		
Työn nimi – Arbetets titel – Title ***Manipulating Thermoresponsive Properties of Polycations in Water***		
Työn laji – Arbetets art – Level ***M.Sc. Thesis***	Aika – Datum – Month and year ***August, 2018***	Sivumäärä – Sidoantal – Number of pages ***61***

Tiivistelmä – Referat – Abstract

This thesis reports the design and study of new series of thermoresponsive polycations with upper critical solution temperature (UCST) and lower critical solution temperature (LCST) type phase separation properties in water.

The polymers were synthesized using reversible addition-fragmentation transfer polymerization process in presence of azobisisobutyronitrile (AIBN) as an initiator and 2-cyano-2 propylbenzoditionate (2-c-2- PBDT) as a chain transfer agent.

Various solution properties of obtained polymers were studied.
Transmittance measurements were utilized to determine the cloud point temperatures of poly[(4-vinylbenzyl)triethyl]ammonium chloride (P-VB-NEt3-Cl), poly[(4-vinylbenzyl)tripropyl]ammonium chloride (P-VB-NPr3-Cl), poly[(4-vinylbenzyl)tributyl]ammonium chloride (P-VB-NBu3-Cl) and poly[(4-vinylbenzyl) tripentyl]ammonium chloride (P-VB-NPen3-Cl) with several counterions (bis(trifluoromethane) sulfonimide, trifluoromethanesulfonate,CH3(CH2)4SO3 and CH3(CH2)11SO3) and anions belonging to Hofmeister series (Cl, NO3, SCN, H2PO4, SO4).
P-VB-NEt3-Cl and P-VB-NPr3-Cl demonstrate both UCST and LCST type phase separation behavior depending on the chosen additive, whereas P-VB-NBu3-Cl and P-VB-NPen3-Cl only show LCST type phase transitions independent of the chosen anions. The phase transition temperature could be manipulated by varying the salt concentration of the polymer solutions; increasing the ionic strength causes the appearence of distinguishable transition in systems with no transition at low ionic strength. Combination of different anions in the system causeseither increase or decrease of the cloud point temperature.
The reversibility of the aforementioned transitions was studied and irreversibility of the transitions of polymersolutions with some anions was determined.
Differential scanning calorimetry measurements were conducted to determine the enthalpy of heating of P-VB-NBu3-Cl and P-VB-NPen3-Cl with specific concentrations of counterions.
Cononsolvency behaviour of P-VB-NBu3-Cl in water/DMF mixtures was studied, indicating that the turbidity occurs due to addition of either of solvents and remains regardless of temperature variation. Particle size measurements were conducted to explain the formation and behavior of particles depending on the temperature variation for P-VB-NBu3-Cl solutions with counterions.

Avainsanat – Nyckelord – Keywords
Polycations, aqueous polymers, LCST, UCST, stimuli-responsive polymers, thermoresponsive polymers, polyelectrolyte, cononsolvency, counterion, Hofmeister series anions, transition reversibility

Säilytyspaikka – Förvaringställe – Where deposited
E-thesis

Muita tietoja – Övriga uppgifter – Additional information

Abbreviations and Symbols

2-c-2-PBDT	2-cyano-2-propylbenzoditionate
AIBN	Azobisisobutyronitrile
ATRP	Atom transfer radical polymerization
CMC	Critical micelle concentration
CRP	Controlled/living radical polymerization
CTA	Chain transfer agent
DMF	Dimethyl formamide
DMSO	Dimethyl sulfoxide
HS	Hofmeister series
IL	Ionic liquid
LCSC	Lower critical solution concentration
LCST	Lower critical solution temperature
$LiNTf_2$	Bis(trifluoromethane) sulfonimide lithium salt
LiOTf	Lithium trifluoromethanesulfonate
micro-DSC	Differential scanning microcalorimetry
NaPS	Sodium 1-pentanesulfonate
NMP	Nitroxide mediated polymerization
NMR	Nuclear Magnetic Resonance
NT	No transition
PDEAm	Poly(N,N-diethylacrylamide)
PDMAEMA	poly(N,N-dimethylaminoethyl methacrylate)
PEI	Poly(ethyleneimine)
PIL	Poly(ionic liquid)
PMVE	Poly (methyl vinyl ether)
PNAGA	Poly (*N* -acryloylglycinamide)
PNIPAm	Poly(N-isopropyl acrylamide)
PNVCL	Poly (N-vinylcaprolactam)
PVAm	Poly(vinyl ammonium)
P-VB-NBu_3-Cl	Poly [(4-vinylbenzyl)tributyl]ammonium chloride
P-VB-NEt_3-Cl	Poly [(4-vinylbenzyl)triethyl]ammonium chloride
P-VB-$NHex_3$-Cl	Poly [(4-vinylbenzyl)trihexyl]ammonium chloride
P-VB-$NPen_3$-Cl	Poly [(4-vinylbenzyl)tripentyl]ammonium chloride
P-VB-NPr_3-Cl	Poly [(4-vinylbenzyl)tripropyl]ammonium chloride
RAFT	Reversible addition fragmentation chain transfer
RT	Room temperature
SDS	Sodium 1-dodecanesulfonate
SFRP	Stable free radical polymerization
T_c^L	Temperature of LCST type phase separation

T_c^U	Temperature of UCST type phase separation
UCSC	Upper critical solution concentration
UCST	Upper critical solution temperature
UV	Ultraviolet
VBA (polymer series)	[(4-Vinylbenzyl)trialkyl]ammonium (polymer series)
ZIP	Zwitterionic polymer

Table of Contents

1. Introduction

This thesis is focused on the synthesis and analysis of thermoresponsive properties of the series of new polycations. This chapter summarizes the literature review of studies of well-known thermoresponsive polymers, and presents a short introduction to the theory and methodology of this research.

1.1. Thermoresponsive polymers in water. Polymers with LCST and USCT behavior

Stimuli-responsive polymers are materials that demonstrate unique properties in a response to several stimuli: temperature, pH, mechanical force, presence of small molecules, electric and magnetic fields [1].

Temperature is one of the most studied types of stimulus affecting the solution behavior of polymers. Properties of thermoresponsive polymers change according to the variation of temperature in solution [2]. This behavior is a key to application of a wide range of aqueous polymers in science and industry. Thermoresponsive polymers have several pharmaceutical and biomedical [3, 4] applications as drug delivery systems, as well as industrial [5-7] applications as water harvesting agents, products for coatings, synthetics *etc*. The utilization of this group of polymers in nanotechnology and catalysis [8] witnesses the significance of stimuli-responsive polymers in science.

Temperature responsivity of the polymer is deduced from the interactions that take place in the system while heating and/or cooling [2, 8]. In aqueous solution, the polymer chain can be in a globular state or a coil state, depending on the polymer-polymer and/or polymer-solvent interactions. If the hydrophobic interactions dominate in the system, the polymer is in globular state; on the contrary, if the hydrophilic interactions supersede the hydrophobic ones, the polymer is in its coil state. This mechanism is crucial in understanding the properties of polymers depending also on pH [9], sensitivity to the light [10, 11], and redox potential [12] change.

According to first observations of thermoresponsive behavior of polymers in solution [13-15], if the system exists as a one phase mixture at low temperatures and, upon increasing, the phase separation occurs, the polymer possesses a lower critical solution temperature (LCST) type behavior. If at low temperatures, aqueous solution of polymer exists as a two-phase mixture, and increasing the temperature results in a complete dissolution of the polymer in water, the polymer is known to have an upper critical solution temperature (UCST) type behavior [2]. LCST and UCST are relatively specific terms that define the exact points of the coexisting curves of the phase diagram of polymers in solution. Only a small range of thermoresponsive polymers show both LCST and UCST type transition. Polymer can be thermoresponsive and not have LCST and/or UCST [13, 14].

1.1.1. Aqueous polymers with LCST-type phase separation behavior

The polymers with LCST-type phase separation have been studied for several decades [13]. Poly(N-isopropyl acrylamide) (PNIPAm) is one of the most studied thermoresponsive polymers with an LCST phase change [14]. This property was discovered in 1968 by Heskins and Guillet [15]. They suggested several theories to explain the behavior of PNIPAm in aqueous solutions. On one hand, the phase separation of PNIPAm can be a result of an entropy effect rising from the formation of hydrophobic bonds (association of the macromolecules between each other). From another theory, the behavior originated from the variation of strength of the hydrogen bonds between the polymer and water molecules upon the temperature change [15].

More studies were conducted to explain the mechanism of the LCST type phase separation behavior [2, 13, 16, 17]. Turbidimetry, calorimetry and light scattering measurements have been used to construct the phase diagram of the polymers in solution. Turbidimetry measurements are useful to detect the temperature of the phase transition for the polymer solution, usually referred to as a cloud point temperature (in the framework of this thesis, T_c). According to Chytrý and Ulbrich [18], the cloud point temperature is not a defined point on the transmittance curve and can vary according to the experiment and the data analyst. Many parameters can affect the transition temperature of the

solution: concentration, molecular weight of the polymer, the presence of additives, heating/cooling rates, etc. [13, 19 - 21]. Calorimetry measurements can detect the temperature of demixing (has the same physical connotation as the cloud point temperature) and the enthalpy of the transition.

It's presumed [2] that the LCST phase separation occurs according to following mechanism. At low temperatures the polymer chain is bound to several water molecules and has a hydrated coil conformation. The elevation of temperature depresses the flexible conformation of the polymer in water, aiming to minimize the contact of polymer with water molecules. This leads to shrinking of the polymer to the globular state. Therefore, the dehydration is the driving force of the phase separation of the LCST type polymers.

The phase separation of the aqueous systems of thermoresponsive polymers was classified by Bergmans and Van Mele [21]. The polymers with a classical Flory-Huggins behavior (type I) [22], the polymers, the chain length of which has no effect to the LCST (type II) [23], and the polymers that present two critical points on the phase diagram (type III), combining the features of type I and type II polymers [24, 25].

PNIPAm. Hofmeister series. Co-non-solvency

Since its discovery in 1956 [14], PNIPAm attracted the attention of many scientists around the world with a unique property of inverse solubility in water and organic solvents upon heating. The LCST phase change was a key in utilizing this polymer and its copolymers as a switching device.

The confirmation of PNIPAm macromolecules in aqueous solutions depends on the hydrogen bonding between the water molecules and nitrogen and carbonyl of the amide group of the repeating unit. Entropy lowers upon mixing due to liberation of the ordered water molecules. This change in entropy leads to increased free energy change and, *ipso facto*, leads to the phase separation.

Heskins and Guillet [15] have used the cloud point method to determine the LCST of PNIPAm: the gradual increase of the temperature of the polymer solution with a known concentration to detect the concentration of the phase transition of the polymer. The application of

several polymer concentrations starting with the highest one not showing a transition until the lowest one showing the transition can give enough information to build a phase diagram of PNIPAm.

Additionally, the aforementioned researchers have carried out calorimetry experiments that were in good agreement with cloud point measurements. The enthalpy of the phase transition is independent of the concentration of polymer, and the endothermic process is a result of weakening of hydrogen bonds between the water molecules and macromolecules [15].

Different additives can be used to alter the LCST type phase transition in the aqueous solutions of PNIPAm [26, 27], although Watanabe *et al.* carried out a research, where they introduced hydrophobic salts into the water solution of PNIPAm. Consequently, an UCST-type phase separation, unconventional to PNIPAm was detected. This phenomenon appears to be dependent on the PNIPAm solubility that can be affected by the variation of solvent Lewis basicity [28].

The addition of surfactants, namely sodium dodecanesulfate (SDS), into the aqueous solutions of PNIPAm [29] leads to the changes in properties of the polymer solution. The addition of 1% SDS to PNIPAm solution will increase the viscosity and decelerate the precipitation. The use of other sodium alkyl salts will affect the LCST of the system [30 - 32], the increase in the concentration of surfactants results in an increased LCST. The size of the precipitated particles decreases below the wavelength of visible light. This phenomenon was later called “intermolecular solubilization” [33].

In the end of 19th century [34] several inorganic salts, later specified as Hofmeister series, were discovered to precipitate certain water soluble proteins. The addition of inorganic salts to aqueous solutions of PNIPAm has been studied by several research groups [35-39]. Cremer *et al.* [36, 37] investigated the effect of anions from the Hofmeister series, proposing the theory that explains the changes in transition temperatures by different mechanisms for different groups of anions, presented below.

$$CO_3^- > SO_4^- > S_2O_3^{2-} > H_2PO_4^- > F^- > Cl^- > Br^- \approx NO_3^- > I^- > ClO_4^- > SCN^-$$

Anions left to Cl^- are referred to as kosmotropes and known as strongly hydrated anions that stabilize macromolecules and have a salting-out effect. Anions to the right of Cl^- have an opposite effect, they are known as chaotropes. Cremer stated, since PNIPAm possesses hydrophobic main chain, hydrophobic isopropyl and amide group, it can interact with anions in three ways. If the anion is binding to polymer through the water molecules, salting-out effect is present. The same effect accompanies modulation of surface tension created by hydrophobic hydration. The other way is direct binding to the amide that should result in salting-in effect [37].

Although, unlike chaotropes, kosmotropes show linear dependency while increasing concentration in relation to the temperature, the transition is observed in a more complicated fashion. Increasing the concentration of kosmotropes in aqueous solutions of PNIPAm will result in a two-step transition. Chaotropes show a non-linear transition with a slight change in temperature upon increase of the concentration. One way or another, presence of anions from HS changes both the LCST and the transition behavior. [36]

One of the unique solution properties of some aqueous polymers is co-non-solvency. This phenomenon occurs when polymer perfectly soluble in two solvents separately, becomes insoluble in the combination of these solvents [40]. This case was observed and studied for PNIPAm in different solvents, altering the logical expectation that the LCST will raise by the addition of a better solvent. When organic solvents are mixed with aqueous solutions of PNIPAm [40], the system shows turbidity. Considering methanol as a second solvent which is capable of bonding to a polymer chain the same way as water molecules, the competitive hydrogen bonding occurs, polymer/methanol and polymer/water. Tanaka et al. [41] use a mathematical approach to describe the phenomenon considering several possibilities of the behavior of solvents' molecules with polymer chains, preferential absorption with a direct site-binding, clustering between methanol and water molecules [42], composition fluctuation of solvents in the mixture [43].

Other neutral thermoresponsive polymers

To this day, PNIPAm is the most studied thermoresponsive polymer [14]. Nevertheless, many other systems have been discovered and studied prior and posterior to PNIPAm. For the biomedical applications, it's preferable for the thermoresponsive polymer to show the transition in aqueous solutions at temperatures between 20°C and 40°C [43]. Poly(N,N-diethylacrylamide) (PDEAm) is one of the alternatives of PNIPAm and shows a phase transition at almost the same temperature range as PNIPAm. Unlike PNIPAm, PDEAm demonstrates lower enthalpy of the phase transition, indicating more lipophilic nature of the latter. This property can be used if the temperature close to physiological is needed [44].

Poly (methyl vinyl ether) (PMVE) is another neutral polymer, temperature-responsive properties of which can be used in various biomedical applications. With a precise transition at 37°C [45], PMVE shows an atypical LCST type phase separation in water, with two lower two-phase areas and an upper area where three phases coexist [46]. Van Durme *et al.* also specify that the increase in the molar mass of the polymer will result in better water solubility. Thus, for shorter polymers the importance of the nature of the end group rises, strongly influencing the LCST.

Poly (N-vinylcaprolactam) (PNVCL) is a second most studied thermoresponsive polymer after PNIPAm, similar to which former shows a reversible LCST type phase separation behavior at temperatures between 30°C and 32°C. Unlike PNIPAm, the polymerization process of PNVCL is much harder to control, therefore the popularity and usage of PNIPAm supersedes these of PNVCL. The study of temperature-dependent properties of aqueous solutions of PNVCL date back to 70s, at about the same time when the similar properties of PNIPAm were reported. The dependence of the cloud point temperature on the molecular weight, rather than the concentration of PNVCL was discovered by Solomon *et al.* [47], but later proved to be untrue [48], both factors affect the phase diagram of aqueous solutions of PVNCL. Regardless the difficulties in synthesis (that have been

solved using novel techniques [49]), PVNCL has a major advantage over PNIPAm; due to its biocompatibility, the environmental applications of PVNCL are expanding day after day.

Many other thermoresponsive polymers have been studied and used for various purposes. Block copolymer of poly(ethylene oxide) and poly(propylene oxide)s, poly(pentapeptide) of elastin and polyacrylamide and interpenetration polymer networks of polyacrylic acid are only a few of the systems with properties comparable to PNIPAm [44].

1.1.2. Aqueous polymers with UCST type phase separation behavior

Only a few polymers have been reported to show UCST type phase separation in aqueous solution [50]. Depending on the type of interactions between macromolecules and solvent molecules UCST can be a result of either Coulomb interactions or hydrogen bonding [51] between the macromolecules and solvent molecules. Commonly known polymers with UCST from hydrogen bonding are poly (ethylene oxide) (PEO), modified poly (vinyl alcohol), poly (hydroxyethyl methacrylate) (PHEMA) *etc.*; PILs and zwitterionic polymers with UCST display Coulomb interactions in the aqueous solutions.

Zwitterionic polymers

Zwitterionic polymers (ZIPs) is a category of macromolecules with an equal number of anions and cations in the polymer chain. Quaternized amines are common as cations, whereas zwitterionic unit often bears a label of anion: sulfobetaine (SB), carboxybetaine (CB) [51].

Thermal response is one of the characteristic features of zwitterionic polymers. Not to be confused with anionic and cationic polyelectrolytes, ZIPs are distinguished by the Coulomb interactions inside the macromolecule as well as between the polymer chains. Large dipole moments and highly charged groups contribute to the distinct hydrophilicity of ZIPs (ionic solvation in water), making them superior in several applications to polyelectrolytes with both hydrophilic and hydrophobic interactions in aqueous solutions [51].

The UCST type phase transition behavior of ZIPs is highly dependent on the molar masses of the polymers. The miscibility range expands when the molar mass increases. The addition of salts to the zwitterionic polymer solutions leads to a disturbance of interactions between ions in the original system. Such additives increase the Debye length (distance at which ions sense each other), increasing the solubility of ZIP in water, in turn lowering the UCST [51].

Antifouling properties make ZIPs appealing for biomedical applications, however lack of biodegradable backbone remains as a main problem for this purpose [52].

UCST based on hydrogen bonding

Much larger group of polymers demonstrates UCST phase separation triggered by hydrogen bonding inside the polymer chains, between them or between the polymer and a solvent. One of the most studied polymers from this group is poly (*N* -acryloylglycinamide) (PNAGA). First synthesized in 1964 [53], PNAGA was found to form gel at a specified temperature. It was stated that thiocyanate and urea prevented gel formation of PNAGA at an original temperature. In water solutions of PNAGA the viscosity increases upon the addition of thiocyanate anions. Gel solutions of PNAGA as well as its several derivatives and copolymers show an UCST type phase separation in water mixtures [51, 54].

Some of the polymers synthesized and analyzed during the present research are polyelectrolytes with UCST type phase transition with certain additives.

1.2. Thermoresponsive polycations

Polyelectrolytes are polymers, repeating units of which carry an ionizable group. If the ionizable group of the repeating unit is a cation, polymer is referred to as polycation; if the group is an anion, polymer is referred to as polyanion [55]. DNA, polypeptides and many other biological macromolecules are polyelectrolytes [56].

In water solution, polyelectrolytes dissociate to form charged polymer chains and small molecular ions of an opposite charge. In this environment, the strong electric interactions occur

between the charged polymer and the counterions, leading to the characteristic properties of polyelectrolytes [55].

Only a few homopolymers carrying ionizable group show LCST type transition behavior [56, 57]. The derivatives of poly(*N*,*N*-dimethylaminoethyl methacrylate) (PDMAEMA), are, probably, the most studied polymers of this class.

1.2.1. PDMAEMA and other weak polycations

The cloud point of an LCST type phase separation of PDMAEMA in aqueous solutions can vary starting from 14°C [58, 59] depending on the molecular weight of the polymer and the pH of the solution. Moreover, different shapes of PDMAEMA results in different types of LCST behaviors. Plamper *et al.* have studied both linear and star-shaped PDMAEMA, revealing that the cloud points of LCST type transitions can be adjusted by varying pH of the system. They have also reported results on obtaining UCST type phase separation in presence of trivalent counterions in aqueous solutions of PDMAEMA [56].

The cloud point of linear and star-shaped PDMAEMA can be adjusted by changing the concentration and molecular weight of the polymer, as well as the pH of the system [57]. The design of the macromolecule doesn't show dependency on cloud point temperature at intermediate and high pH.

Thermoresponsive properties of PDMAEMA can be manipulated by introducing the hydrophobic anions [60]. These properties have been discussed thoroughly in section 1.2.3.

Other poly(*N*,*N*-dialkylaminoethyl methacrylates) show properties of stimuli-responsive polycations. Aqueous solutions of poly(*N*,*N*-diethylaminoethyl methacrylate) [61] and poly(*N*,*N*-diisopropylaminoethyl methacrylate) [62, 63, 64] show LCST-type phase separation as well as sensitivity to pH.

Other weak polycations, poly(ethyleneimine) (PEI), poly(vinyl amine) (PVAm) and poly(allylamine hydrochloride) or chitosan fail to show similar behavior as PDMAEMA and its

derivatives. However, they have been used in creating new copolymers with polyanions, properties of which reveal interest to this class of polymers. [55]

1.2.2. Strong Polycations

Aqueous solutions of a strong polycation, Poly(tributyl-4-vinylbenzylphosphonium pentanesulfonate), shows a reversible LCST type phase transition. Depending on the concentration of the polymer and the presence of additives, the cloud point temperature of this polycation can be tuned in wide temperature range [65]. Its various derivatives (depending on the length of the phosphonium and sulfonate carbon chains) also show LCST type phase separation [66]. These polymers were further used in synthesis and characterization of nanoparticles.

1.2.3. Effect of counterions on the thermoresponsive behavior of polycations

As it was discussed earlier, addition of hydrophobic counterions to the system with polycations changes their thermoresponsive behavior and can lead to the appearance of UCST type phase transition in LCST characteristic system. Hydrophobic anions (bis(trifluoromethane) sulfonamide (NTf_2) in particular) form ion pairs with repeating units of polycation and increases its basicity, in turn decreasing the solubility of the system. The UCST behavior can be observed if the system has a sufficient ionic strength. Buffering the solution can provide the sufficient ionic strength to observe the behavior. Therefore, the effect of the counter ion is vastly dependent on the pH of the system [60].

The derivatives of PDMAEMA have also shown change in the thermoresponsive behavior by introducing the hydrophobic anions, in this case both bis(trifluoromethane) sulfonamide (NTf_2) and trifluoromethanesulfonate (OTf) [67]. The addition of smaller anions to the system results in increase of the ionic strength, hence better reciprocation of the UCST type phase transition.

1.3. Controlled Radical Polymerization

Radical polymerization is a set of the most utilized techniques in production of vinyl homo and copolymers. Several controlled radical polymerization (CRP) methods are employed to obtain

polymers with specific features: stable free radical polymerization (SFRP), atom transfer radical polymerization (ATRP) and reversible addition fragmentation chain transfer (RAFT) are the most commonly used techniques [68].

Nitroxide mediated polymerization (NMP) is the SFRP method [68], where nitroxide radicals control the growth of the polymer chain by reversible capping and de-capping. This method helps to slow down the process and decrease the concentration of growing radicals, reducing the number of side reactions and resulting in narrow molecular weight distributions [69].

Since its discovery, ATRP technique has gained more interest, compared to other CRP techniques. Control over the polymerization of different monomers, resulting in achievement of different kinds of polymer architectures (block, graft, stars, combs, *etc*.) is the main advantage of ATRP [70]. Additionally, RAFT is a versatile method used with wider range of monomers than other CRP methods [71].

1.3.1. Reversible addition-fragmentation chain transfer.

The significance of RAFT polymerization is the use of chain transfer agents (CTA). The most frequently used CTAs modern polymer chemistry are xanthates, dithiobenzoates, trithiocarbonates, dithiocarbamates. CTA is often chosen depending on the monomer to be used in the polymerization process. The mechanism of RAFT is presented on scheme 1.3.1. Firstly, the initiator is activated forming a radical (I) that interacts with monomer (II). Then, monomers keep reacting with newly formed monomer radical forming a polymer chain radical. When the polymer chain radical meets a CTA, the radical is transferred from polymer chain to the tail of CTA (III), forming a new radical. One chain of the polymer is formed with a thiocarbonyl end group. The new radical can reciprocate step II forming another polymer (IV), or terminate (VI). Another possibility is that step IV polymer can interact with a polymer with end group to reach an equilibrium state (V) [72].

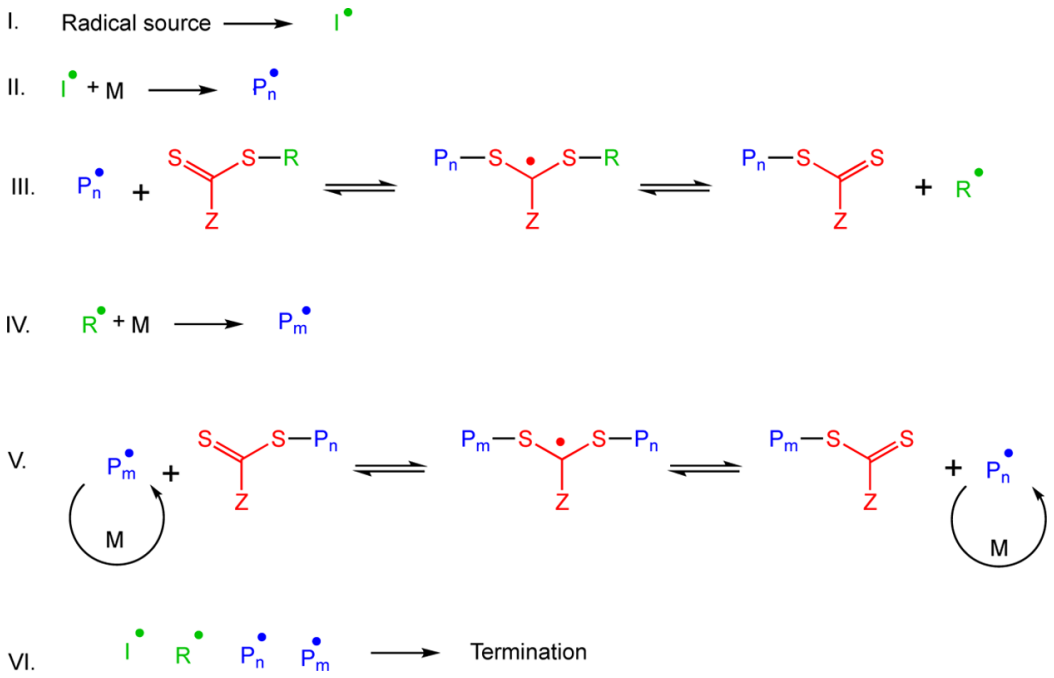

Scheme 1.3.1. Proposed mechanism of RAFT [72]

A unique feature of RAFT polymerization is use of CTA that retains in the product of reaction, therefore keeping the polymer in its dormant state, so that the polymer can be used in synthesis of block copolymers and end-functional polymers. The drawback of the presence of thicarbonylthio group is the need for further treatment in its removal in some cases [71].

2. Experimental part.

2.1. Materials

4-Vinylbenzyl chloride (Aldrich, 90%, 500 ppm tertbutyl catechol as inhibitor), 2-cyano-2-propylbenzoditionate (Aldrich, 97.0% HPLC grade), azobisisobutyronitrile (Fluka, 99.0% purum. recrystallized from methanol), triethylamine (Merck KGaA, 99.0% GC), tripropylamine (Aldrich, 98.0%), tributylamine (Fluka, puriss. p. a. ≥99.0% GC), triamylamine (TCI, 98.0%), trihexylamine (Aldrich, 96.0%), lithium trifluoromethanesulfonate (Aldrich, 96%), bis(trifluoromethane) sulfonimide lithium salt (Aldrich, purics. ≥99% (^{19}F NMR)), monohydrate of sodium 1-pentanesulfonate (Alfa Aesar, HPLC grade), dodecane sulfate sodium (Merck KGaA, 2 phase titration ≥99%), NaCl (Fischer, an. reag. grade 99.98%), $NaNO_3$ (VWR, 99%), $NaH_2PO_4*2H_2O$ (VWR, 99%), NaSCN (Aldrich, 99%), anhydrous Na_2SO_4 (Fischer, lab. reag. grade 99%), HCOONa (Aldrich, 99%), dimethylsulfoxide (Fischer, HPLC grade 99.98%), acetone (Aldrich, HPLC grade 99.8%), diethyl ether (VWR, 100%) were used as received. N, N - dimethylformamide (Fluka, HPLC grade, purum. >99%) was distilled under reduced pressure and dried over molecular sieves (3Å, VWR). Deuterated solvents used for NMR measurements D_2O (99.96%), MeOD (99.8%), CD_3Cl (99.90%) were produced by Eurisotop.

2.2. Instrumentation and sample preparation

Nuclear Magnetic Resonance.

The NMR measurements were performed on Bruker Avance III 500 MHz spectrometer. ^{1}H NMR was used for the monomer, polymer and conversion analyses of all the products obtained from the reaction. ^{1}H NMR was also used for the temperature measurements of a few samples to determine and follow the phase transition phenomenon. For these measurements the samples were prepared using 5 mg of polymer (the bigger amount of polymer was used to increase the intensity of polymer peaks on the NMR spectrum), the salt (NaCl) of appropriate concentration and 1 mg of

sodium formate (HCOONa), D_2O was used as a solvent for the closest comparison to transmittance measurements.

Differential Scanning microcalorimetry (micro-DSC).

Calorimetry measurements were performed on Microcal PEAQ-DSC instrument to determine the enthalpy of the phase transition of the polymer solutions. 1 ml of water samples with 1mg/ml polymer concentration and an appropriate salt concentration were used, the samples were cooled and degassed right before introducing to the instrument. The temperature range between 5 and 85°C was set. The heating rate for all experiments was set to 60°C/hr, the stabilization time was 5 minutes before the heating. Reference was deionized water. The determination of enthalpy of transition and the temperature of the maximum heat capacity is shown using the reference subtracted and baseline corrected heating curve on fig. 2. 1. 1.

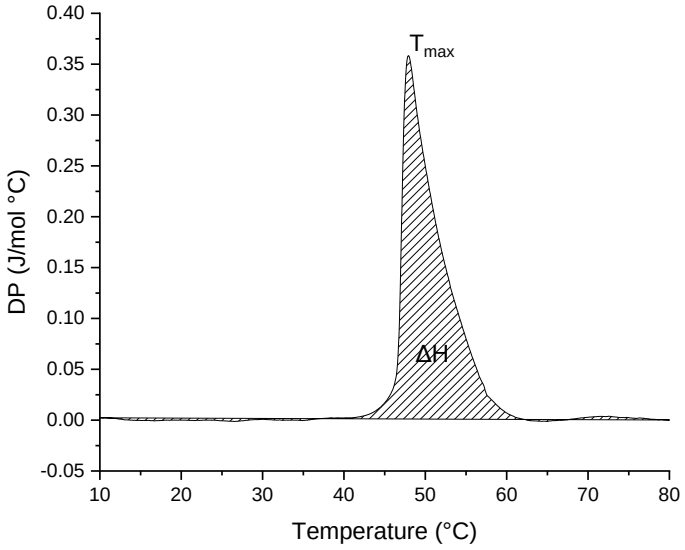

Fig. 2.1.1. Determination of the temperature of maximum heat capacity and enthalpy of transition.

ZetaSizer.

Particle size measurements were performed on Z-Sizer Nano for several samples showing the transition with a starting transmittance being lower than the transmittance of water. The temperature range between 15 and 90°C was set. Three measurements with two minutes stabilization time at each temperature were performed. The water samples of 2 ml were prepared in 3 ml glass cuvettes. The appropriate concentrations of salts were used with 1mg/ml polymer concentration. Intensity and

volume average sizes through the diameter of particles were used in the results and discussion section.

Transmittance measurements.

The transmittance measurements were performed on Jasco V-750 Spectrophotometer and Jasco J-815 CD Spectrometer. 2.5 ml water samples were prepared in 3 ml glass cuvettes with appropriate concentration of salt(s) and 1mg/ml of the polymer. The samples showing LCST type phase transitions were cooled down to 5°C and left at this temperature for at least one hour before the measurement. Both UCST and LCST systems were degassed right before the measurement. Prior to the analysis the samples were equilibrated for 10 or 5 min at the start temperature depending on the instrument in use. The temperature range between 5°C and 90°C was set for the heating and cooling measurements, with a temperature rate of 1°C/min. The cloud points were determined as demonstrated on fig. 2. 1. 2. The same approach was used for UCST type transitions.

Determination of number average molecular mass

Jasco V-750 Spectrophotometer was used in determination of number average molar mass of the polymers. The wavelength range was set between 400 and 190 nm with data interval of 0.5 nm, the temperature was set to 23°C. Polymers were dissolved in filtered methanol in concentrations of approximately 1 mg/ml. The CTA was dissolved in buffer in nine different concentrations to determine the extinction coefficient.

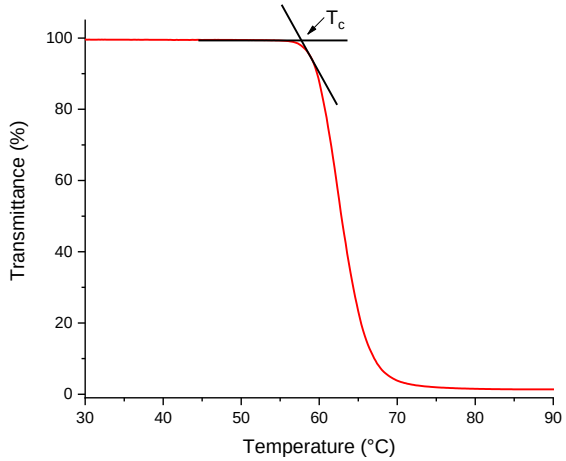

Fig. 2.1.2. Determination of a cloud point temperature as example on an LCST type phase transition curve.

2.3. Syntheses

All polymers were synthesized following the same protocol. First, the monomer was synthesized using 4-vinylbenzyl chloride and an appropriate amine, then the monomer was introduced into the reversible addition-fragmentation chain transfer polymerization reaction in organic solvent with a chain transfer agent and an initiator.

[(*4-Vinylbenzyl)tributyl]ammonium chloride* was synthesized from 4-vinylbenzyl chloride and tributylamine via amine quaternization reaction. 4-vinylbenzyl chloride (100 mmoles, 14.456 g) and tributylamine (130 mmoles, 25.319 g) were mixed with 50 ml acetone in 250 ml round-bottom flask. The reaction was performed in 40°C preheated oil bath for 24 hrs. The resulting monomer was precipitated using diethyl ether (2 L) and dried in the vacuum desiccator for 4 hrs at 50°C.

Poly [(*4-Vinylbenzyl)tributyl]ammonium chloride* was synthesized from [(4-Vinylbenzyl)tributyl]ammonium chloride via RAFT polymerization. [(4-Vinylbenzyl)tributyl]ammonium chloride (30 mmoles, 10 g), azobisisobutyronitrile (0.17 mmoles, 4.1 mg) and 2-cyano-2-propylbenzodothionate (1.5 mmoles, 36.1 mg) were dissolved in 15 ml of distilled and dried dimethylformamide. The nitrogen bubbling was used for the oxygen isolation. The reaction was left in 100°C preheated oil bath for 23 hrs. The reaction was stopped by freezing using liquid nitrogen bath. Dialysis was performed in MWCO 3500 dialysis tubes right from the reaction

mixture in deionized water for 5 days (the water in beaker was changed once/twice a day), followed by the freeze-drying of the water solution.

[(*4-Vinylbenzyl)tripentyl]ammonium chloride* synthesized from 4-vinylbenzyl-chloride and tripentylammonium following the same protocol as for the previous monomer. The same procedure was used for the [(*4-Vinylbenzyl)triethyl]ammonium chloride*, [(*4-Vinylbenzyl)tripropyl]ammonium chloride* and [(*4-Vinylbenzyl)trihexyl]ammonium chloride* monomers.

The polymerization processes of [(*4-Vinylbenzyl)tripropyl]ammonium chloride*, [(*4-Vinylbenzyl)tripentyl]ammonium chloride and* [(*4-Vinylbenzyl)trihexyl]ammonium chloride* also represent the polymerization of the [(*4-Vinylbenzyl)tributyl]ammonium chloride.* Due to extremely low solubility of [(*4-Vinylbenzyl)triethyl]ammonium chloride* monomer in DMF, the solvent of its polymerization process was replaced with DMSO.

3. Results and discussion.

3.1. Polymerization process

The structures and corresponding names of all the obtained polymers are presented on fig. 3.1.1. Four out of five synthesized polymers were soluble in water. Poly [(4-vinylbenzyl)trihexyl]ammonium chloride (P-VB-NHex$_3$-Cl) was the only water-insoluble polymer from the series; this property eliminated the analytical aspect of the study of this polymer, limiting it to ^{1}H NMR structure characterization. Although, P-VB-NHex$_3$-Cl formed a stable colloidal suspension in water/DMF solution, making dialysis and further treatment possible.

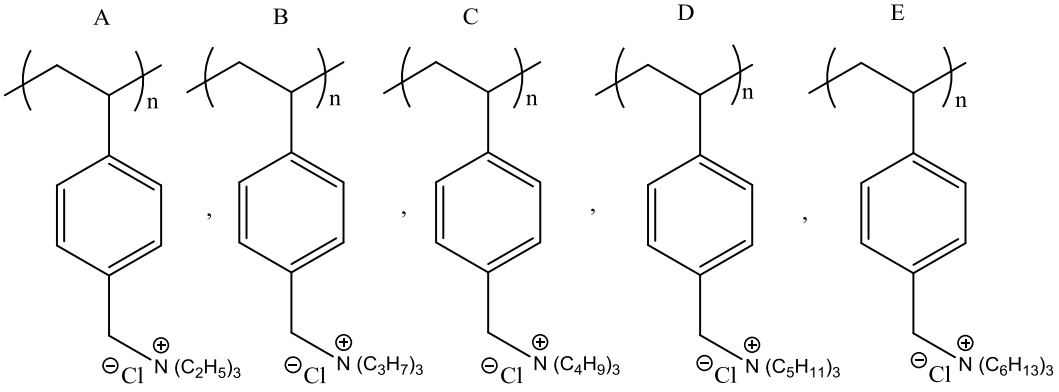

Fig. 3.1.1. Structures of the synthesized polymers: A) P-VB-NEt$_3$-Cl, B) P-VB-NPr$_3$-Cl, C) P-VB-NBu$_3$-Cl, D) P-VB-NPen$_3$-Cl, E) P-VB-NHex$_3$-Cl

Table 3.1.1. The yields of all experiments and conversions of the polymerization reactions.

Monomer	yield, %	yield, g	
VB-NEt3-Cl	43	11	
VB-NPr3-Cl	31	4.6	
VB-NBu3-Cl	33	11	
VB-NPen3-Cl	30	5	
VB-NHex3-Cl	43	12	
Polymer	yield, %	yield, g	conversion, %
P-VB-NEt3-Cl	44	4.8	76
P-VB-NPr3-Cl	46	2.1	77
P-VB-NBu3-Cl	44	4.5	82
P-VB-NPen3-Cl	14	0.6	96
P-VB-NHex3-Cl	55	6.5	55

The conversions and yields of the synthesized polymers as well as the yields of the reactions of synthesis of monomers are presented in table 3.1.1. Low yield of P-VB-NPen3-Cl was obtained due to mechanical difficulties in handling the polymer.

The syntheses of the VBA polymer series follows the same scheme presented on fig 3.1.2. The monomer was synthesized from 4-vinylbenzyl chloride and tertiary amine. The reversible addition/fragmentation transfer (RAFT) polymerization reaction was conducted using azobisisobutyronitrile (AIBN) as a radical initiator and 2-cyano-2-propylbenzoditionate (2-c-2-PBDT) as a chain transfer agent.

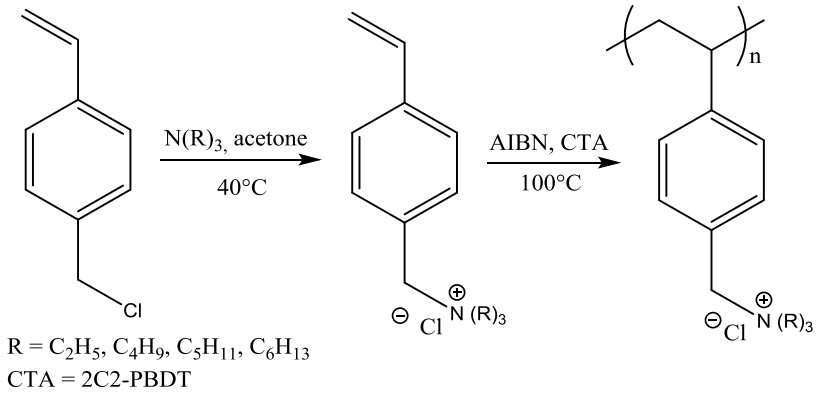

Fig. 3.1.2. The scheme of the reactions used to synthesize VBA polymer series

The ^{1}H NMR spectra presented in Appendixes 1-5 were used to examine the structures of polymers and follow the intensity dependency on the length of the alkyl tails. Peaks of solvents with corresponding protons marked in black are assigned, as well as the protons of polymers.

Table 3. 1. 2. Number average molar masses of polymers

Polymer	experimentally obtained M_n, g/mol	Theoretical M_n, g/mol
P-VB-NEt_3-Cl	34 200	44 500
P-VB-NPr_3-Cl	38 400	45 900
P-VB-NBu_3-Cl	61 800	50 400
P-VB-$NPen_3$-Cl	69 100	72 100

Size Exclusion Chromatography [73] is widely used technique to determine the molecular weights and distributions of polymers. The complications in performance of this measurement (the

polymer, probably, stayed in the column and did not elute with DMF/LiBr, H_2O/LiBr buffer solutions) with VBA polymer series was a reason to pursue Ultraviolet/visible (UV/vis) spectroscopy instead. The masses of polymers determined by UV spectroscopy are presented in Table 3.1.2. and compared to theoretical molar masses of the polymers, determined using the formula below [74].

$$M_n\ (theor) = M_{CTA} + \frac{[Mono]}{[CTA]} \times M_{Mono} \times Con_p$$

where M_{CTA} and M_{Mono} are molar masses of CTA and monomer, respectively; *[Mono]* and *[CTA]* are concentrations (in moles) of monomer and CTA used in polymerization reaction, respectively. Con_p is a conversion of the polymerization reaction.

UV spectra of the CTA, polymers and corresponding monomers are presented in fig. 3.1.3. (a). The absorbance of polymers and CTA at 310 nm were considered in further calculations, since this is one of the wavelengths, where the signals of monomers and CTA do not overlap. Fig. 3.1.3 (b) shows the absorbance-concentration dependency of CTA used for determination of extinction coefficient (ε), deduced using Beer-Lambert law:

$$A = \varepsilon\, b\, c$$

where *A* is absorbance, *b* is path length and *c* is the concentration of CTA.

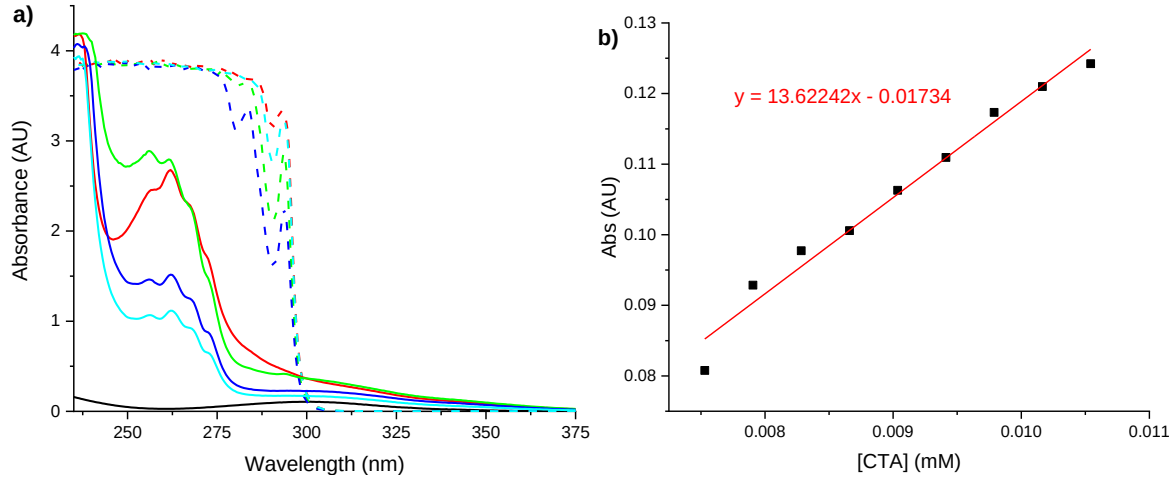

Fig. 3.1.3. a) UV spectra of CTA (black), P-VB-NEt$_3$-Cl (red), P-VB-NPr$_3$-Cl (green), P-VB-NBu$_3$-Cl (blue) and P-VB-NPen$_3$-Cl (light blue) are presented in solid lines, corresponding monomers bare same colors presented with dashed lines. b) Dependency of absorbance at 310 nm on the concentration of CTA (■) and fitted trendline with formula (in red).

Afterwards, the extinction coefficient was used to find molar concentration of the polymer in the system. The assumption was that the extinction coefficients of CTA and polymer end-groups are equal and all of the polymers in the system contain end-groups.

The aqueous polymers synthesized during this research were used in various analytical approaches to investigate the thermoresponsive and solution properties. None of the polymers show thermoresponsive behavior in pure water, however the addition of several anions causes the appearance of turbidity upon the temperature variation.

3.2. Thermoresponsive behavior of the VBA polymer series with counterions

The aqueous solution properties of the polymers described in this section were studied in presence of four different salts: lithium trifluoromethanesulfonate (LiOTf), bis(trifluoromethane) sulfonimide lithium salt ($LiNTf_2$), sodium 1- pentanesulfonate (NaPS) and sodium dodecanesulfonate (SDS). The choice of salts was based on previously studied [65, 67, 75] effects of hydrophobic anions to thermoresponsive properties of polycations in water solutions. The behavior of polymers from VBA series was compared to a well-known set of thermoresponsive polymers, the possible differences were determined and discussed.

3.2.1. P-VB-NEt_3-Cl

Poly[(4-vinylbenzyl)trietyl]ammonium chloride (P-VB-NEt_3-Cl) was the most hygroscopic polymer of the series. The tests included use of counterions such as OTf and NTf_2 in presence of NaCl. No transition behavior was observed with NaPS.

The presence of OTf anions in the aqueous solutions of P-VB-NEt_3-Cl results in appearance of an UCST type phase transition and the graph presented on fig. 3.2.1. reflects the dependency of the UCST type phase transition cloud point temperature (T_c^U) on the concentration of OTf anions. Comparing to the previous studies of polycations such as poly(2-(methacryloyloxy) ethyltrimethylammonium iodide) (PMOTAI) [60] and PDMAEMA [67] with OTf anions, much

smaller amount of OTf is needed to detect the first transition of the system in present case. Temperature measurements of aqueous solutions of PMOTAI [60] in presence of OTf anions first shows a rapid increase of the cloud point temperature with increasing the concentration of LiOTf. The dependency changes after reaching a certain salt concentration, and T_c^U starts decreasing, when the concentration increases. The aqueous solutions of P-VB-NEt_3-Cl only show increase of T_c^U with increasing the concentrations of OTf. At concentrations of OTf higher than 30 mM, the system with P-VB-NEt_3-Cl starts forming aggregates. The difference between PMOTAI and P-VB-NEt_3-Cl might occur due to differences in the structures of the repeating units, strength of the interactions between the polycation and the counterion and/or other electrostatic interactions in the system.

When introduced into water, P-VB-NEt_3-Cl dissociates, forming positively charged P-VB-NEt_3^+ polymer chains and small negatively charged Cl^- ions. When the LiOTf is introduced into water, it also dissociates to form positive Li ions and negative OTf ions. When the two systems combine, OTf anions substitute the Cl anions and form ion pairs with positively charged repeating units of polymer chain, and the water-insoluble P-(VB-NEt_3^+ $^-$OTf) polymer precipitates. Increasing the temperature of the system will result in dissociation of P-(VB-NEt_3^+ $^-$OTf) and, therefore, release of the P-VB-NEt_3^+ and OTf anions to water.

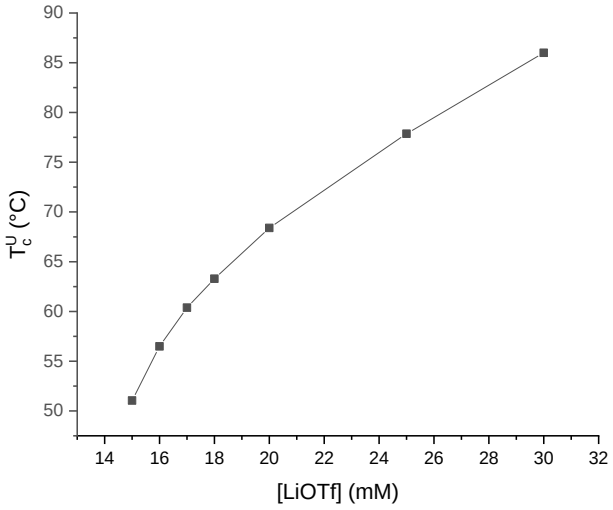

Fig. 3.2.1. Cloud point temperature of 1 mg/ml P-VB-NEt_3-Cl aqueous solutions as function of LiOTf concentration

The analysis of thermoresponsive properties of P-VB-NEt_3-Cl in presence of $LiNTf_2$ did not show distinguishable transitions. At low concentrations of $LiNTf_2$, while the aqueous system is still clear, no transition is observed. When the concentration of anions is increased, the system becomes turbid before the heating and shows no transition during turbidimetry measurements. This behavior was previously observed with the same counterion for aqueous solutions of PMOTAI [60]. The origin of this phenomenon was related to the insolubility of the PMOTAI-NTf_2 system. The addition of smaller anions resulted in distinguishable transitions.

The appearance of turbidity of aqueous solutions of P-VB-NEt_3-Cl with $LiNTf_2$ upon increase of concentration at room temperature is observed. Cooling or heating of the system did not result in dissolution of the precipitate. Instead, gel-like particles were formed at temperatures above 90°C. The author suggests, the non-thermoresponsive phase separation occurs from precipitation of polymer-NTf_2 system. As it was the case with LiOTf anions, the P-(VB-NEt_3^+ $^-NTf_2$) is water insoluble. On the other hand, from the structure of $LiNTf_2$ [76], there is a free electron pair on the nitrogen that can form donor-acceptor bonds with atoms that have valent orbitals or δ+ (hydrogen atoms of water molecules) or systems with positive charge (P-VB-NEt_3^+ in this case). If this is the case, the system becomes sterically stable, therefore rising the temperature (from 5 to 90°C) will not result in breaking of the bond. This description of the phenomenon can explain the formation of gel-like particles at temperatures above 90°C and the lesser concentration of $LiNTf_2$ (compared to LiOTf) needed for the first appearance of turbidity.

Similar to PMOTAI [60] and PDMAEMA [67], the addition of NaCl in presence of NTf_2 anions results in a clear transition. Unlike PMOTAI, P-VB-NEt_3-Cl presents ability to show both UCST and LCST type phase transition at specific concentrations of NTf_2 (Fig. 3.2.2. a).. Due to irregular type of behavior, instead of plotting the cloud point temperature as function of

concentration of NTf_2 anions, author prefers to present the temperatures at transmittance minima of the transition curves as function of the NTf_2 anions concentration (3.2.2.b).

Theories discussed for PDMAEMA [67] and PMOTAI [60] can explain the behavior of NaCl and $LiNTf_2$ in aqueous solutions of P-VB-NEt_3-Cl. Addition of NaCl increases the ionic strength of the system, allowing the polymer to show LCST type phase transition. Additionally, author proposes explanation of the UCST type behavior of P-VB-NEt_3-Cl. From the measurements of P-VB-NEt_3-Cl solutions solely in presence of NTf_2 anions, the phenomenon of non-thermoresponsive phase separation was discussed. Although, the phases are separated, positively charged P-VB-NEt_3 polymer chains are still present in water solution. When NaCl is introduced the concentration of Cl anions in the system increases, consequently, Cl and NTf_2 anions compete to bind the rest of the positively charged P-VB-NEt_3 polymer chains. At low temperatures, the contribution of Cl anions overbalance the contribution of NTf_2 anions (the clouds of Cl anions shield the polymers from NTf_2) and more P-VB-NEt_3-Cl polymers present in the system, hence the transmittance is increased. The heating results in dissociation of newly formed P-VB-NEt_3-Cl polymers and contribution of NTf_2 anions overbalances, hence the transmittance lowers. The balance is depressed again when the temperature is increased above the T_{min} , and the contribution of Cl anions overbalances the contribution of NTf_2.

Further cooling of the aqueous solutions of P-VB-NEt_3-Cl with Cl/NTf_2 only presents an UCST type phase separation (3.2.2.a). This phenomenon might be related to solution properties of P-VB-NEt_3-Cl, which shows a clear UCST transition with other anions (NaSCN, LiOTf), although transition solely in NaCl was not detected, as well as in other anions (except NaSCN) of Hofmeister series. Author suggests that notwithstanding the ability to show LCST type seraration, the UCST type phase transition is more likely to be observed for P-VB-NEt_3-Cl with several anions. The

presence of LCST type behavior is more pronounced for other polymers of VBA series and this phenomenon is discussed thoroughly in the comparisons part of this chapter.

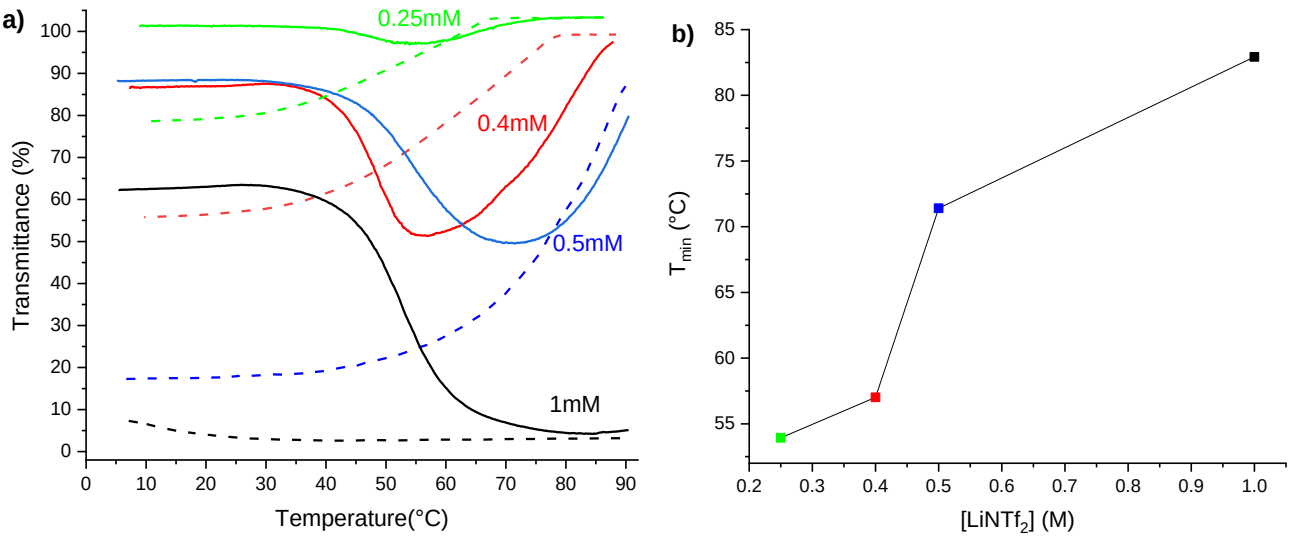

Fig. 3.2.2. a) Transmittance curves as function of temperature of 1mg/ml P-VB-NEt_3-Cl in 0.5 M NaCl and various color-coded concentrations of $LiNTf_2$. Solid lines - heating, dashed lines – cooling.
b) Temperature at transmittance minima of the transition curves as function of the NTf_2 anions concentration at constant concentration of NaCl (0.5M)

No transition appeared from the addition of different concentrations of sodium pentanesulfonate to aqueous solutions of P-VB-NEt_3-Cl.

3.2.2. P-VB-NBu_3-Cl

Poly[(4-vinylbenzyl)tributyl]ammonium chloride (P-VB-NBu_3-Cl) was the most studied polymer from the VBA polymer series. The experiments with its solution properties included use of NaPS, NaCl, SDS and $LiNTf_2$. NaPS and $LiNTf_2$ were chosen to compare the properties of P-VB-NBu_3-Cl to properties of cationic polyelectrolytes [65, 67] studied prior to this research. SDS was chosen to see if the longer alkyl chain of sulfate (compared to NaPS) will give different results.

With the aforementioned counterions P-VB-NBu_3-Cl shows an LCST type phase separation, although different types of transitions were observed. The effect of SDS (Fig. 3.2.3. a) shows the formation of particles before the heating. Hydrophobicity of the long alkyl chain is, most probably, the reason for the early particle formation. This behavior might be a result of cooperative binding

[77, 78] that occurs when a molecule prefers to attach next to a unit that is already attached to another molecule of the same nature. In this case it's more favorable for a dodecane sulfate anion to bind to the unit near a unit already bonded with dodecanesulfate. When only one part of the polymer chain keeps binding with a bulky dodecanesulfate anion, the particles will form at low temperatures. The particle formation will start at a very low concentrations of SDS prior to the heating process. When the concentration of SDS increases the system becomes more turbid. The ability of dodecanesulfate anions to show LCST type phase separation is due to coagulation of the formed particles. The cloud point temperature of the LCST type phase transition is decreasing when increasing the concentration of SDS (fig. 3.2.3.b) until 2mM. In more concentrated solutions the transmittance drops below 5%, but the cloud point temperature slowly increases.

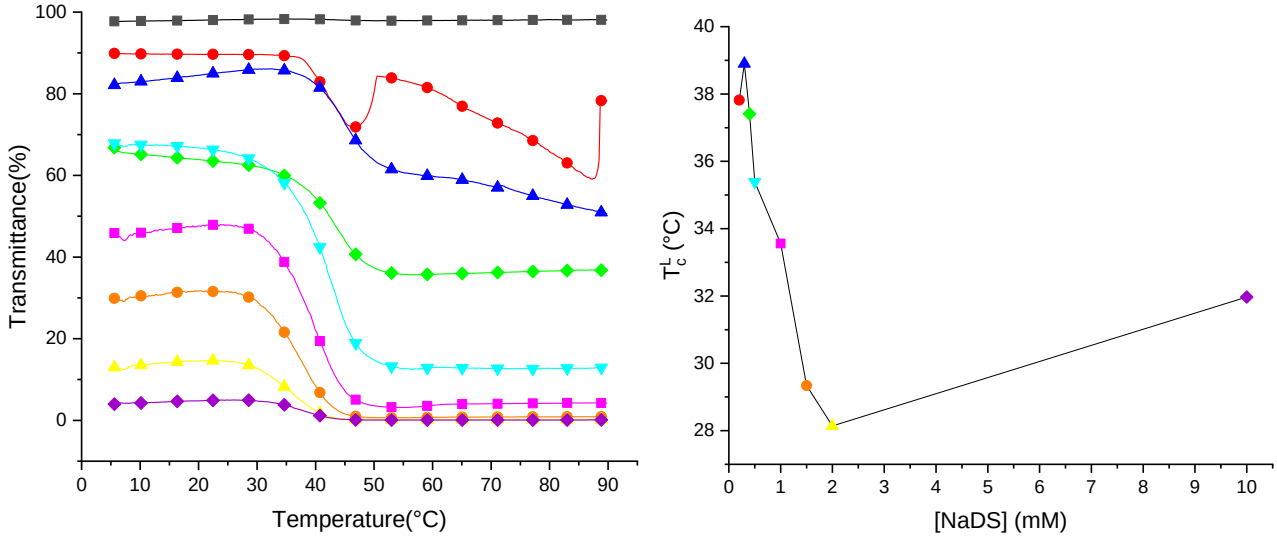

Fig. 3.2.3. a) Transmittance curves as function of temperature of 0.1 mM (■), 0.2 mM (●), 0.3 mM (▲), 0.4 mM (♦), 0.5 mM (▼), 1mM (■), 1.5mM (●), 2mM (▲), 10mM (♦) of SDS in 1mg/ml aqueous solutions of P-VB-NBu_3-Cl. For easier interpretation, every 11^{th} symbol is presented.
b) Cloud point temperature as function of the concentration of SDS for 1mg/ml aqueous solutions of P-VB-NBu_3-Cl

To inspect the phenomenon of particle formation prior to the heating and during the heating process, the particle size measurements were conducted while increasing the temperature of the system. The typical size distribution chart is shown on the fig. 3.2.4. for the sample before the transition temperature at 15 and 40°C and after the transition temperature at 75°C. Both volume and intensity average particle sizes are presented.

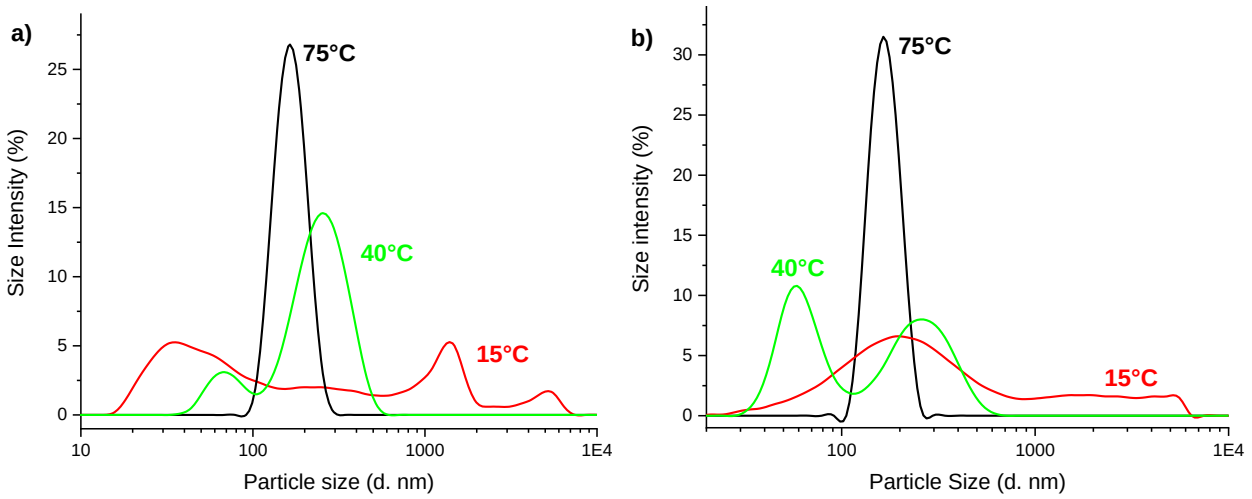

Fig. 3.2.4.a) Intensity and b) volume average size distribution chart for different temperatures of the 0.4 mM concentration of SDS samples in 1 mg/ml aqueous solutions of P-VB-(NEt_3)-Cl

At low temperatures (15°C), particles of three or four different size distributions are present in the mixture. At (or slightly higher) transition temperatures (40°C), particles with two different size distributions can be observed in the system. After the transition temperature (75°C), particles of only one size distribution are present. The author proposes following explanation: at low temperatures polymer chains bound to dodecane sulfate anions form water-insoluble particles; elevation of temperature causes the water-insoluble particles to reduce their surface area and coagulate.

From the data presented on fig. 3.2.5., one can evaluate intensity and volume average particle size distribution upon the temperature variation. Before the transition temperature, the size distribution appears to be quite wide. It narrows down after the transition temperature. Particles above 3000 nm in diameter is most likely the dust, however the regular appearance of these particles for all the different concentrations of SDS might be an evidence of a different origin - polymers with DS anions attached. More particles appear at the lower size range (between 5 and 500 nm). The distribution for all the cases (3.2.5 a-d) narrows down to about 200 nm for both volume and intensity average. A slight increase of average particle size can be observed above 75°C, which is far away from the transition temperature of presented systems. In this case, probability that certain temperature affects the aggregation of formed micelles in solution is high. The polymer chains in the system are of different length. It's only logical that the corresponding hydrophobic polymers will

also have different length, hence different particle size. As discussed in a previous paragraph, the coagulation of particles with various lengths of the polymer chain will reach an equilibrium after the transition is complete, therefore the distribution narrows down to smaller particle size.

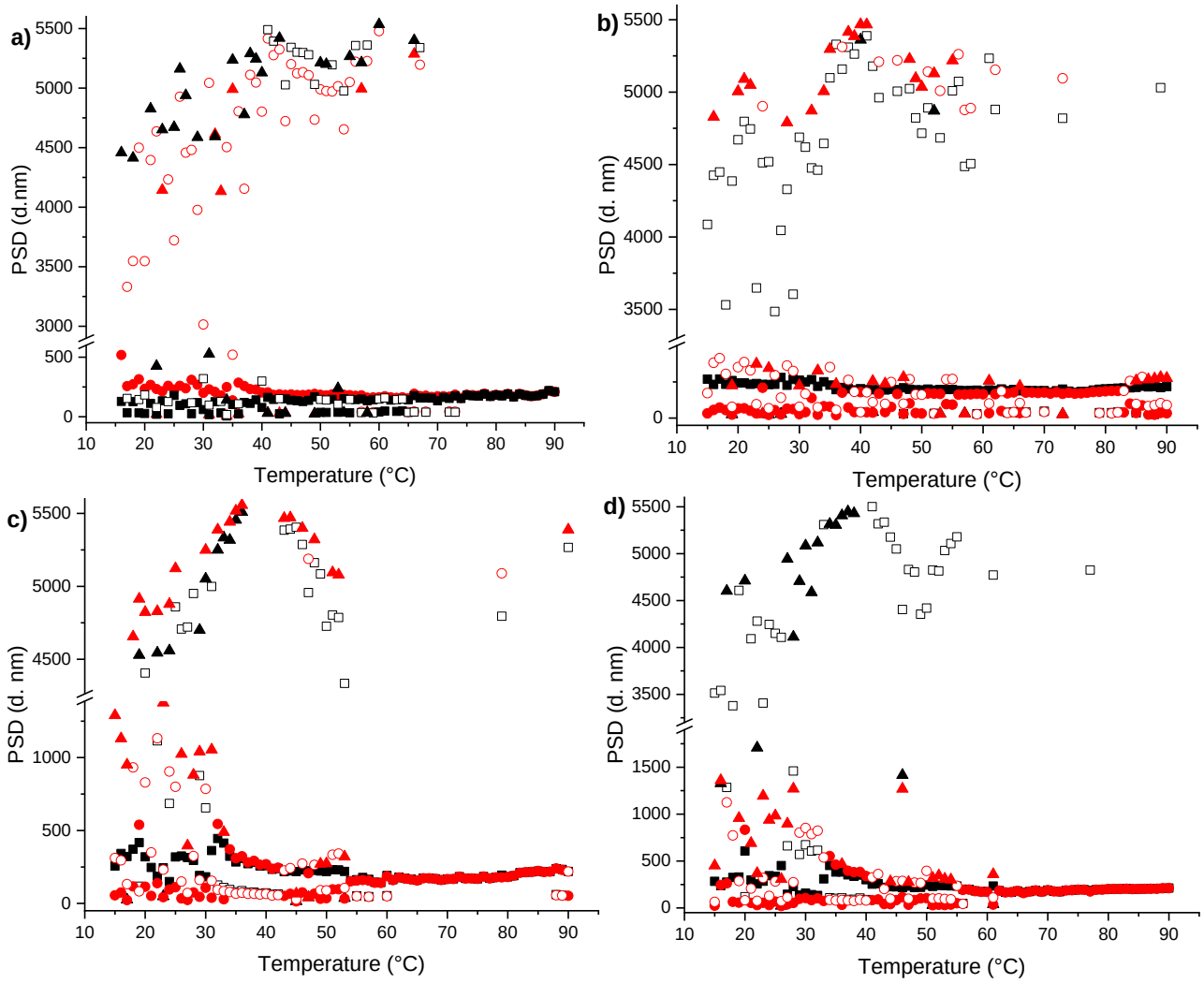

Fig. 3.2.5. Volume (in red) and intensity (in black) average diameter of the particles as function of temperature with SDS concentrations of a) 0.2 mM, b) 0.3 mM, c) 0.4 mM and d) 0.5 mM in 1 mg/ml solution of P-VB-NBu$_3$-Cl. Different symbols represent different peaks of the particle size distribution. The break on the Y axis is introduced to skip the empty area of the graph.

The difference between effects of SDS and NaPS is significant. In water solutions of P-VB-NBu$_3$-Cl pentanesulfonate anions demonstrate a typical LCST phase separation. Fig. 3.2.6. shows phase diagram of P-VB-NBu$_3$-Cl depending on concentrations of NaPS and NaPS in 0.25 M NaCl, indicating the decrease of the cloud point of an LCST type phase separation (T_c^L) upon increase of

ionic strength of the system, nevertheless the concentration that shows the lowest T_c^L (lower critical solution concentration (LCSC)) of NaPS remains the same (0.4 M).

The shape of the curve before LCSC is relatively similar to shapes of temperature-concentration curves of inorganic salts (section 3.2.2.). The increase of cloud point temperature in concentrations above LCSC might be an evidence of surfactant-like binding of PS anions to the polymer. Although this phenomenon has been observed for years [2, 13, 79, 80], no explanation was proven to this day.

Calorimetry measurements were conducted for several samples showing distinct transitions with NaPS and NaPS/NaCl solutions to examine enthalpy and difference in transition temperatures of heating and cooling processes. Relatively unusual dependency of enthalpy of heating on transition temperature partially resembles the temperature/concentration graph from fig. 3.2.6. The phenomenon seems to represent the hydrophobic hydration [81], when the water molecules gather around the hydrophobic molecules allowing Van der Waals interactions. This clustering of water molecules around hydrophobic anions causes increase in enthalpy that can be observed on fig. 3.2.7.b

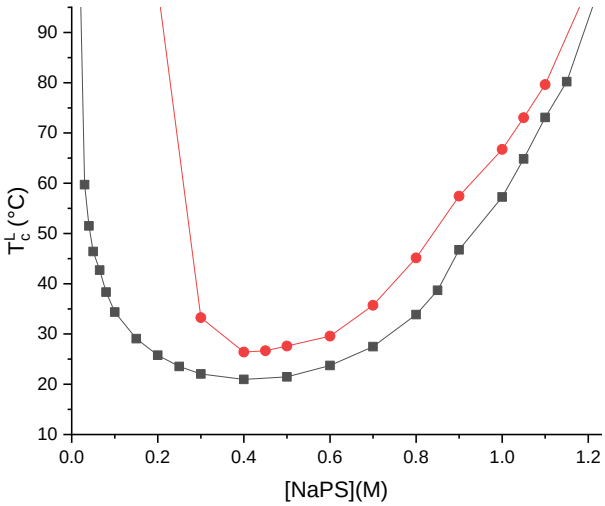

Fig. 3.2.6. Cloud point temperature as a function of concentration of NaPS with (●) and without (■) addition of 0.25 M NaCl in aqueous 1 mg/ml solutions of P-VB-NBu$_3$-Cl.

The transition of the cooling process of 0.7 M concentration of NaPS in aqueous solution of P-VB-NBu$_3$-Cl was split and showed two peaks relatively close to one another (on fig. 3.2.7. two □

symbols at concentration 0.7 M). The phenomenon was observed before [82, 83], and appears to be an evidence of presence of the "glassy" state of the system.

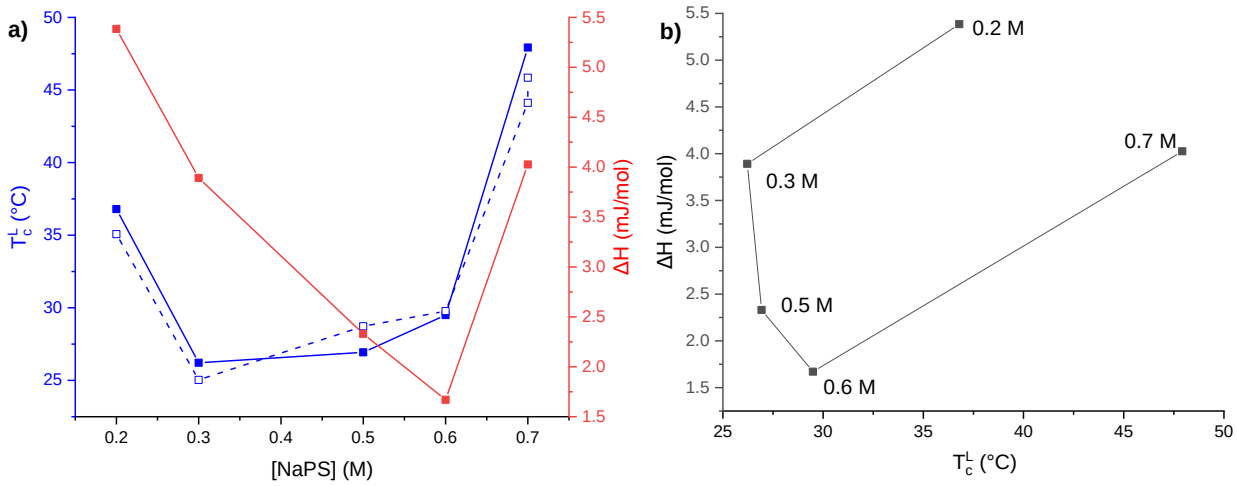

Fig. 3.2.7. a) Cloud point temperature and enthalpy of heating as functions of concentration of NaPS in 1mg/ml aqueous solutions of P-VB-NBu$_3$-Cl. Solid blue line (■) follows heating, dashed line (□) follows cooling procedure.b) Enthalpy of heating as function of temperature for NaPS

The exponential decrease followed by a sharp increase of the enthalpy corresponds to LCST type behavior of polymer-PS system. Since the dependence of concentration of NaPS on the temperature cannot be characterized as a regular phase diagram, the terms LCST and LCSC were chosen to represent the distribution in an understandable manner. Addition of NaCl to the system with NaPS shows a stable decrease of the enthalpy of heating in concentrations below 0.4 M (Fig. 3.2.8. a), while the cloud point temperature decreases. The concentrations below and above the presented ones in fig 3.2.7 and 3.2.8. were not taken into account, since they did not show distinguishable peaks.

From both 3.2.7. a and 3.2.8. a graphs, a very significant difference in cooling and heating T_{max}/T_{min} can be observed. According to literature [81], the temperature of demixing should appear lower in the reverse process. In present case, for both NaPS and NaPS/NaCl systems, this parameter fluctuates (appears higher at some points of concentrations and lower at other points).. The cooling and heating rates were the same, but the effect of thermal history during cooling process might prevent the regular nature of thermal hysteresis.

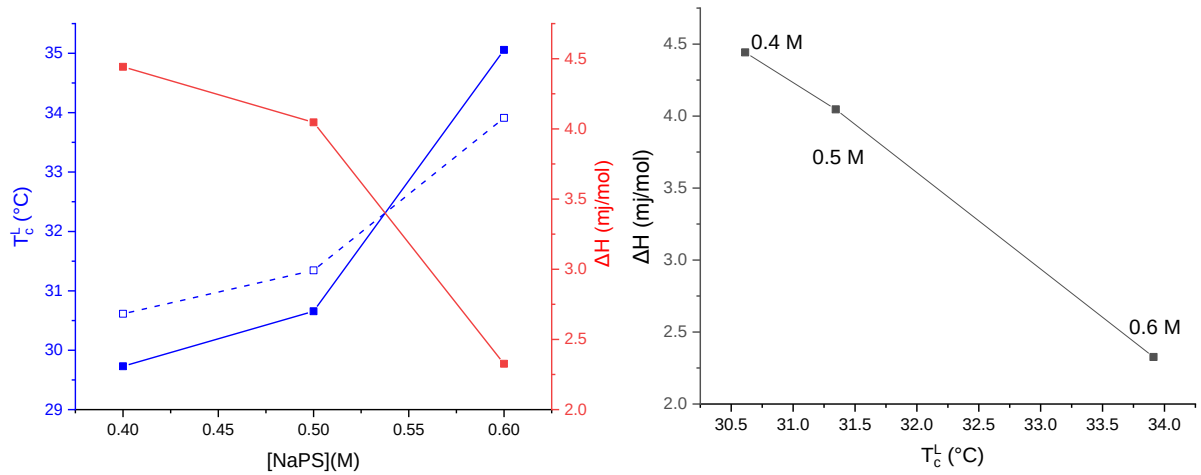

Fig. 3.2.8. a) Cloud point temperature and enthalpy of heating as functions of concentration of NaPS in 1mg/ml aqueous solutions of P-VB-NBu$_3$-Cl. Solid blue line (■) follows heating, dashed line (□) follows cooling procedure.
b) Enthalpy of heating as function of temperature for NaPS in 1mg/ml aqueous solutions of P-VB-NBu$_3$-Cl.
Concentration of NaCl for all points of both graphs is equal – 0.25 M.

The transitions in presence of $LiNTf_2$ salts in water solutions of P-VB-NBu_3-Cl was complicated to analyze. Therefore, increase of ionic strength was used to determine if distinct transitions can be observed. As in case with P-VB-NEt_3-Cl, constant concentration of NaCl was used, while varying the concentration of $LiNTf_2$ (Fig. 3.2.9).

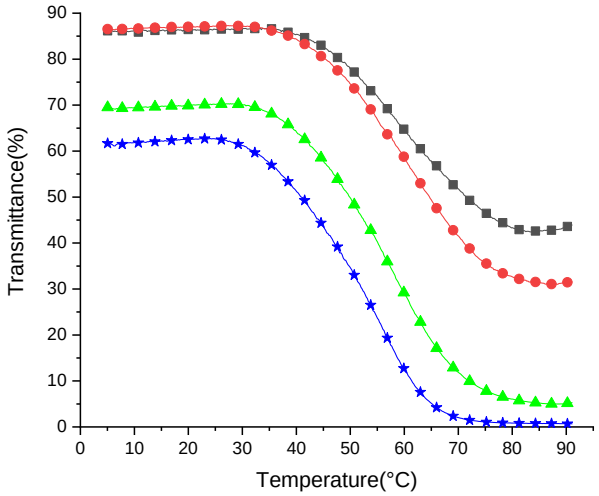

Fig. 3.2.9. Transmittance curves as functions of temperature with equal concentration of NaCl (0.5 M) and 0.3mM (■), 0.5 mM (●), 0.7 mM (▲), 1mM (★) concentrations of LiNTf$_2$ in 1 mg/ml water solutions of P-VB-NBu$_3$-Cl. For easier interpretation, every 11th symbol is presented.

The similarity between the transition patterns of $LiNTf_2$/NaCl and SDS measurements might be a result of equivalent mechanisms of transitions. As it was observed with aqueous solutions of P-VB-NEt_3-Cl and $LiNTf_2$, the precipitation of the polymer starts before the heating process. Particle

size measurements for different concentrations of $LiNTf_2$ (Fig. 3.2.10) display several types of distributions with increasing the temperature.

In case of low concentrations of $LiNTf_2$ (0.3 mM), at low temperatures there are three groups of particles of different size with a distribution between 0 and 5500 nm. When temperature is increased, the particle size distribution narrows down to ~200 nm. The phenomenon is similar to the one observed for P-(VB-NBu_3-DS) system. The particles are of different size and elevated temperature causes polymers to aggregate and decrease the surface area of the hydrophobic P-(VB-NBu_3-NTf_2).

In case of higher concentrations of $LiNTf_2$ (0.7 mM), at low temperatures there are three groups of particles of different size as in previous case. Here, the temperature elevation causes the distribution to split to particles of small size (~200 nm) and particles of bigger size (1500-5000 nm). This might be a consequence of cross-linking with formation of gel-like particles, as it was discussed earlier for P-(VB-NEt_3-NTf_2) systems. NTf_2 anions act as cross-linkers between the two polymer chains resulting in formation of gel-like particles at high temperatures that will show bigger article size.

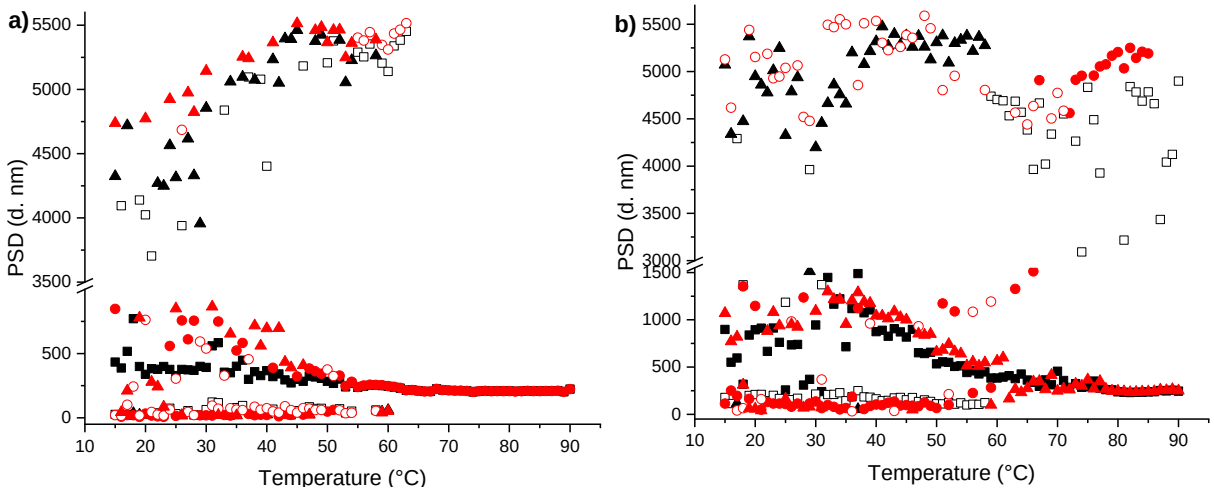

Fig. 3.2.10. Volume (in red) and intensity (in black) average diameter of particles as function of temperature with $LiNTf_2$ concentrations of 0.3 mM (a) and 0.7 mM (b) in 1 mg/ml solution of P-VB-NBu_3-Cl. The concentration of NaCl in both experiments was equal – 0.5 M. Different symbols represent different peaks of the particle size distribution. The break on the Y axis is introduced to skip the empty area of the graph.

The presented results of analysis of P-VB-NBu_3-Cl with several counterions indicate that P-VB-NBu_3-Cl acts as an LCST system in combination with several counterions, and its properties can be regulated by addition of appropriate anions. Two different types of LCST transitions were observed: LCST, where the system is one-phase in temperatures below the T_c^L and a two-phase in temperatures above the T_c^L (the case with NaPS and NaPS/NaCl additives); and an LCST, where the system is two-phase below the T_c^L, though the transition still appears.

3.2.3. P-VB-$NPen_3$-Cl

The poly[(4-vinylbenzyl)tripentyl]ammonium chloride (P-VB-$NPen_3$-Cl) was soluble in water only to limited extent. Measurements of thermoresponsive properties of P-VB-$NPen_3$-Cl with sodium pentanesulfonate (NaPS) only in presence of NaCl (Fig. 3.2.11) were possible. Solely in presence of NaPS and with other counterions the same behavior was observed as in case with $LiNTf_2$ and aqueous solutions of P-VB-NEt_3-Cl, proving again that sufficient ionic strength is needed to observe a thermoresponsive phase transition. The transition dependency of NaPS/NaCl with this polymer is nowhere near the dependency observed for P-VB-NBu_3-Cl.

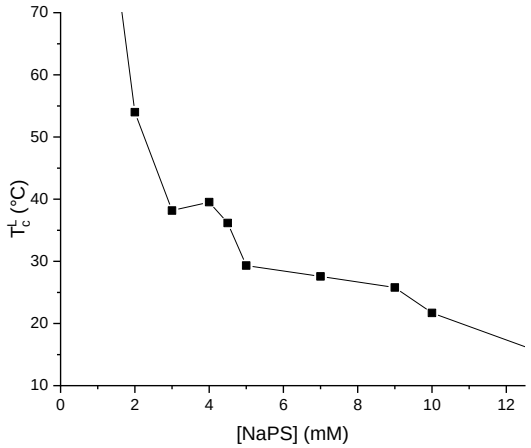

Fig. 3.2.11. Cloud point temperature as a function of concentration of NaPS with 0.1 M NaCl in aqueous 1 mg/ml solutions of P-VB-$NPen_3$-Cl.

In NaPS/NaCl combination the aqueous solutions of P-VB-$NPen_3$-Cl show an LCST type phase separation and the exponential decrease of T_c^L while increasing the concentration. The nature of an uncharacteristic pattern at concentration 4 and 4.5 mM of NaPS might be due to the presence of

the coagulation. Microcalorimetry measurements were conducted with the same range of concentrations (Fig. 3.2.12), showing relatively linear increase of enthalpy of heating by increasing the concentration of NaPS. Unlike the calorimetry measurements of P-VB-NBu_3-Cl with the same counterion, heating/cooling transition temperatures in case with P-VB-$NPen_3$-Cl follows the rules of thermal hysteresis [82].

Although, P-VB-$NPen_3$-Cl was one of the least studied polymers of the VBA series, its analysis helped in understanding of transition dependency of LCST-type phase separation of VBA systems.

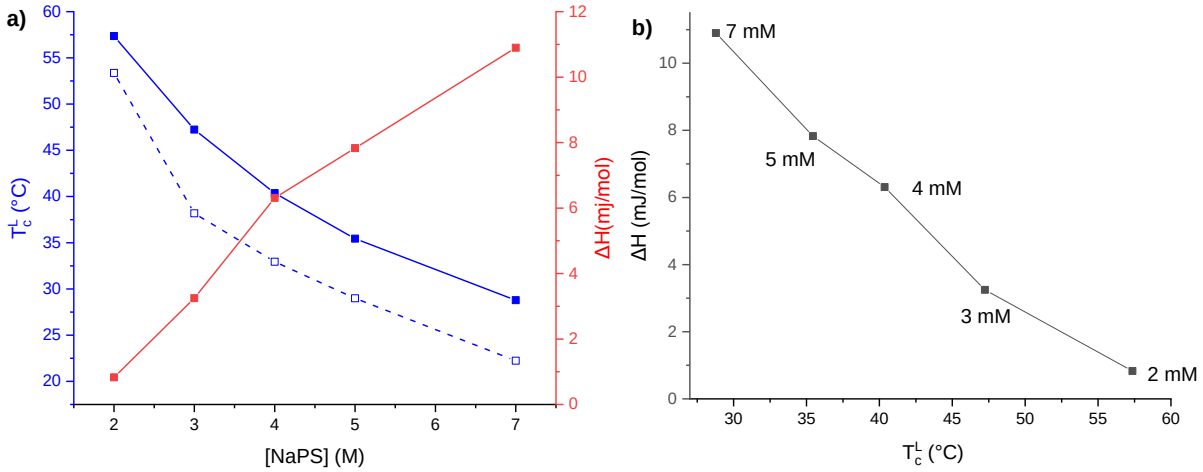

Fig. 3.2.12. a) Cloud point temperature and enthalpy of heating as functions of concentration of NaPS in 1mg/ml aqueous solutions of P-VB-$NPen_3$-Cl in presence of 0.1 M NaCl. Solid blue line (■) follows heating, dashed line (□) follows cooling procedure. b) Enthalpy of heating as function of temperature for NaPS in 1mg/ml aqueous solutions of P-VB-$NPen_3$-Cl in presence of 0.1 M of NaCl.

3.3. Hofmeister series

The effect of some anions from the Hofmeister series in relation to the aqueous solutions of polymers was studied. Not all polymers from VBA series show distinct transitions with HS anions. Table 3. 3. 1 summarizes the effects of considered anions that show differently characterized transitions. Normal LCST transition, where the solution is absolutely clear at low temperatures and rapidly turns turbid after the cloud point temperature, is marked on the table as $LCST^1$. As it was in case with $LiNTf_2$ and P-VB-NEt_3-Cl, some anions show turbidity at RT or below, but the phase transition can still be observed, this kind of transition is marked as $LCST^2$. Other unusual transition

behavior is marked as LCST[3]. This was observed only for nitrate anions with P-VB-NBu_3-Cl and will be discussed in an appropriate section.

Table 3.3.1. Transition dependency of polymers regarding chosen HS anions

Polymer	reaction to SO_4^{2-}	reaction to $H_2PO_4^-$	reaction to Cl^-	reaction to NO_3^-	reaction to SCN^-
P-VB-NEt_3-Cl	NT	NT	NT	NT	UCST
P-VB-NPr_3-Cl	NT	NT	LCST[2]	LCST[2]/UCST	LCST[2]/UCST
P-VB-NBu_3-Cl	NT	LCST[2]	LCST[1]	LCST[3]	NcT
P-VB-$NPen_3$-Cl	LCST[1]	LCST[2]	LCST[1]	NcT	NcT

Introducing anions to aqueous solutions of polymers doesn't always result in transition. This case is marked as NT (no transition). When the transition doesn't occur at low concentrations before the mixture becomes two-phased is marked NcT (no clear transition).

3.3.1. P-VB-NEt_3-Cl

One of the first salts to be tested with P-VB-NEt_3-Cl was NaCl. In 1mg/ml aqueous solutions of P-VB-NEt_3-Cl NaCl did not show any traceable transitions up until concentrations of 5.9 M. Since the solubility of NaCl in water is limited (6.2 M) [83], solutions with higher concentrations were complicated to obtain. Tests with Na_2SO_4, NaH_2PO_4 and $NaNO_3$ were performed as well, no transition was observed.

The only anion from HS capable of providing results was NaSCN. The addition of NaSCN at concentrations between 15 and 45 mM shows UCST type phase separation. At concentrations above 45 mM bigger particles appear at RT that do not dissolve at 90°C or above, forming aggregates instead (Fig. 3.3.2). Unlike, P-VB-NEt_3-Cl shows an UCST by the addition of NaSCN, though the dependency of T_c^U on the NaSCN concentration looks similar to the T_c^L dependency of PNIPAm [36]. The gap between the two T_c^U is much wider in case with P-VB-NEt_3-Cl.

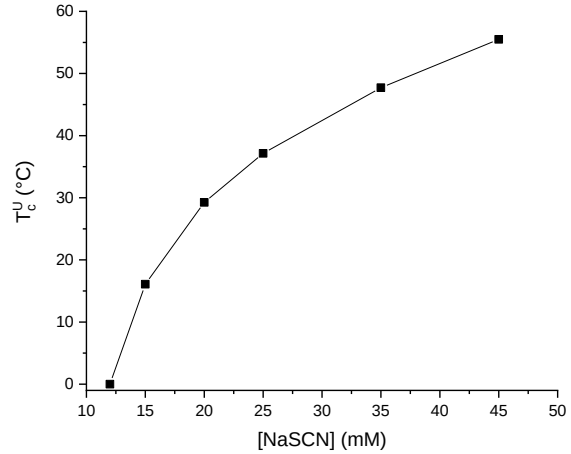

Fig. 3.3.1. Cloud point temperature of a UCST type phase separation as a function of NaSCN concentration in aqueous 1 mg/ml solutions of P-VB-NEt$_3$-Cl

The response of 30 mM solutions of NaSCN in P-VB-NEt$_3$-Cl to addition of several concentrations of urea was considered (Fig. 3.3.2). The decline of UCST was observed.

Urea is known to increase the solubility of proteins by disrupting the non-covalent interactions. It's possible that this phenomenon is observed in the case with NaSCN solutions of P-VB-NEt$_3$-Cl. Introduction of urea into the system breaks the ionic interactions between SCN^- and ammonium units, instead forming hydrogen bonds with the polymer. Increasing the concentration of urea will decrease the cloud point temperature of the system with a constant concentration of SCN^- anions.

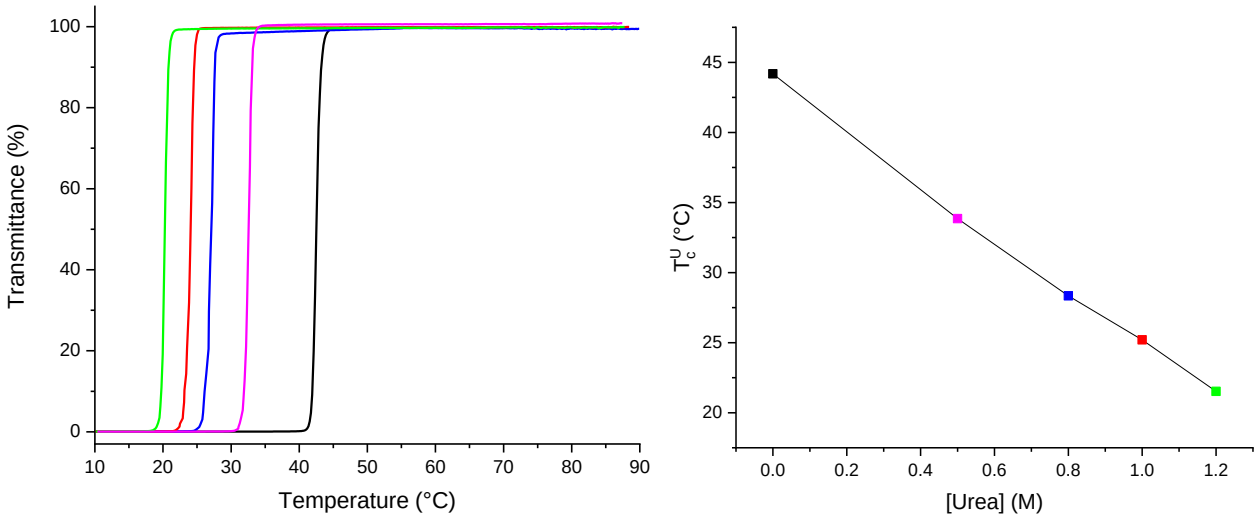

Fig. 3.3.2. a) Transmittance curves as a function of temperature for 30 mM concentration of NaSCN samples with no urea (in black), 0.5 M (in pink), 0.8 M (in blue), 1 M (in red) and 1.2 M (in green) of urea in 1mg/ml aqueous solution of P-VB-NEt$_3$-Cl. b) Cloud point temperature of a UCST type phase separation as a function of concentration of added urea with a constant concentration of NaSCN (30 mM)

3.3.2. P-VB-NPr_3-Cl

Several anions from HS were used to examine the thermoresponsive properties of poly[(4-vinylbenzyl)tripropyl]ammonium chloride (P-VB-NPr_3-Cl) in water solutions. As it was indicated in Table 3.3.1., the combination of aqueous solution of P-VB-NPr_3-Cl and NaCl show an LCST type phase separation (Fig. 3.3.3). Very high concentrations of NaCl were necessary for the system to show the first transition (3.25 M), which was not complete at 90°C. Unlike P-VB-NBu_3-Cl and P-VB-$NPen_3$-Cl, temperature transitions of NaCl solutions of P-VB-NPr_3-Cl weren't as sharp (3.3.3. left) and the transmittance at RT slightly decreased by the addition of Cl anions. The highest concentration of added NaCl was 5.5 M, further addition of anions resulted in formation of aggregates upon heating, that did not completely dissolve after the cooling procedure. Linear decrease of the cloud point temperature upon addition of NaCl is comparable to the previously studied LCST polymers [35, 36].

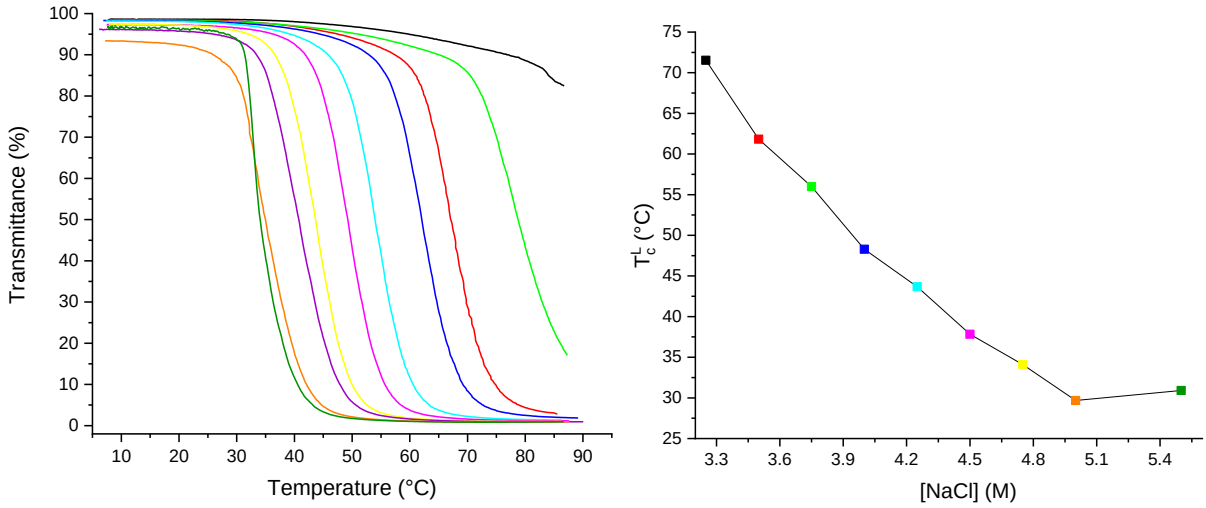

Fig. 3.3.3. Transmittance curves as function of temperature (left) and cloud point temperature of LCST type phase separation as a function of NaCl concentration (right) in aqueous 1 mg/ml solutions of P-VB-NPr_3-Cl

The reaction of P-VB-NPr_3-Cl to NaSCN anions show both LCST[2] and UCST type phase separation (Fig. 3.3.5). The observation of LCST was relatively easy, though very narrow range of concentrations showed a distinguishable cloud point temperature. Taking concentrations of NaSCN higher than 8mM shows instant turbidity at RT that doesn't clear out at lower temperatures. Addition

of urea though resulted in the first distinguishable appearance of UCST along with LCST. Addition of urea increases the diaphanousness of the mixture shifting from 60 to 70% transmittance. This behavior allows usage of NaSCN concentrations higher than 8 mM, but with appropriate concentration of urea. As it was discussed earlier in section 3.3.1. urea and SCN anions compete to bound to ammonium groups. As this phenomenon was previously discussed in case with Cl anions addition to system with NTf_2 and water solutions of P-VB-NEt_3-Cl. The present observation is the result of the same kind of phenomenon. Only urea doesn't affect the ionic strength of the system, it only forms hydrogen bonds with polymer chains and competes with other anion.

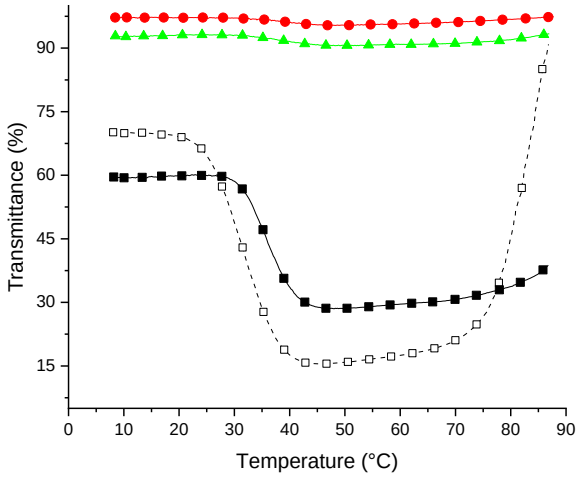

Fig. 3.3.5. Transmittance curves as a function of temperature for concentrations of NaSCN 5 mM (●), 7 mM (▲), 8 mM (■) and 8 mM with the addition of 1 M of urea (□) 1mg/ml aqueous solution of P-VB-NPr_3-Cl. For easier interpretation, every 15th symbol is presented.

It was easier to observe both LCST and UCST type transitions with $NaNO_3$ in aqueous solutions of P-VB-NPr_3-Cl, much wider concentration range was applied to receive results on Fig. 3.3.6. The unusual LCST type phase transition was observed, indicating presence of particle before the cloud point temperature. UCST type phase separation, on the other hand showed barely visible double transition with only a slight difference from one another at 200 mM and lower (Fig. 3.3.6 a). Cooling curves of the same concentrations of $NaNO_3$ did not resemble the reverse of the heating curves, indicating that LCST separation process is partially irreversible. The LCST here looks like a type III demixing [84].

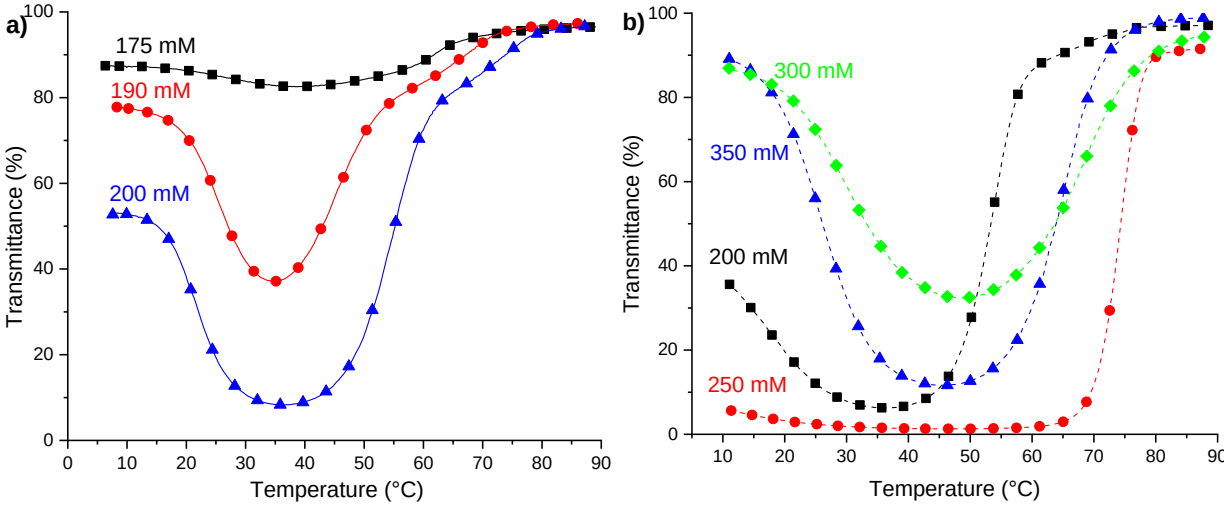

Fig. 3.3.6. a) Heating curves as a function of temperature for 175 mM (■), 190 mM (●) and 200 mM (▲) concentrations of $NaNO_3$ in 1mg/ml aqueous solution of P-VB-NPr_3-Cl. b) Cooling curves as a function of temperature for 200 mM (■), 250 mM (●), 300 mM (♦) and 350 mM (▲) concentrations of $NaNO_3$ in 1mg/ml aqueous solution of P-VB-NPr_3-Cl. For easier interpretation, every 15th symbol is presented.

3.3.3. P-VB-NBu_3-Cl

Reaction of P-VB-NBu_3-Cl to anions of HS was unlike the reaction of any other thermoresponsive polymers. The results do not agree with commonly approved patterns in case of PNIPAm and many other LCST systems [19].

For Cl^- anions a very clear set of transitions appeared in a wide range of concentrations of NaCl (Fig. 3.3.7). These results were also used to perform other tests with NaCl. ^{1}H NMR analysis (Fig. 3.3.8) was in a good agreement with the turbidity measurements.

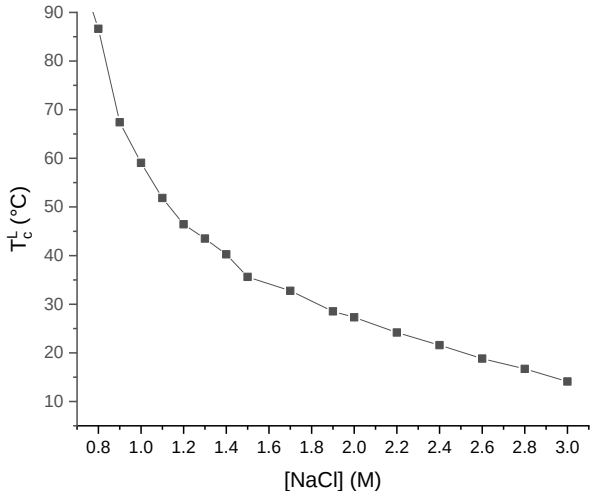

Fig. 3.3.7. Cloud point temperature as a function of NaCl concentration in aqueous 1 mg/ml solutions of P-VB-NBu_3-Cl

According to NMR measurements of hydrogels of PNIPAm [85] at different temperatures, the dehydration and eventual collapse of hydrogels occurs at elevated temperatures. This observation was the driving force to investigate the dehydration of aqueous systems of P-VB-NBu_3-Cl in presence of NaCl with increasing the temperature. The intensities of signals corresponding to different functional groups of the polymer decreases with increasing the temperature. The integrals of the different functional groups appears to differ when changing the solvent. The integrals of different functional groups of P-VB-NBu_2-Cl in D2O indicating that different groups are dehydrated differently.

Relative intensities of the ^{1}H NMR signals of three concentrations of NaCl (a)1M, b)1.5 M, c) 2M) as a function of temperature show sharp transitions in aqueous solutions of P-VB-NBu_3-Cl. Two stages of transition can be observed on fig. 3.3.8.a. First stage, between temperatures 5 and 60°C is a plateau, meaning no dehydration happens at this temperature range. Second stage witnesses rapid dehydration of propyl tails of ammonium and slight dehydration of aromatic groups and alpha-CH_2 groups of P-VB-NEt_2-Cl. The same ratio of the different functional groups that contribute to the dehydration is observed for two other concentrations of NaCl. Three stages of transition can be observed on fig. 3.3.8.b and c. In case of 1.5 M NaCl dehydration starts at 5°C (stage 1) and accelerates after reaching the phase transition temperature (stage 2) until 60°C. From 60°C to 82°C and higher the third stage appears as a plateau, referring to absence of dehydration. In case of 2 M NaCl first stage ($5<T<25$) as well as third stage ($T>55$) witness absence of dehydration and the second stage between 25 and 55°C shows rapid dehydration. The concentration of NaCl has a major influence on the dehydration of the polymer chains. The phenomenon of more significant dehydration of alkyl chains is due to the bigger size of this group compared to other two.

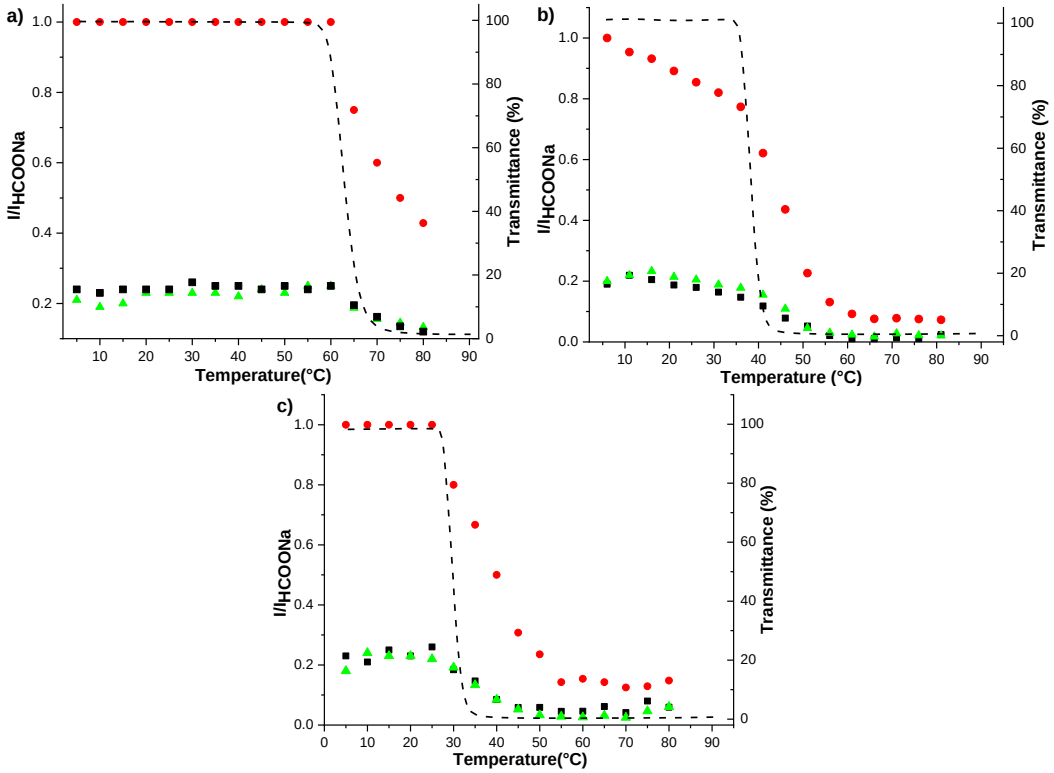

Fig. 3.3.8. Dependency of intensities of ^{1}H NMR signals of P-VB-NBu$_3$-Cl on temperature. Protons of propyl tails (●), α-CH$_2$ groups of ammonium (■) and aromatic protons (▲) of 5 mg/ml D$_2$O solutions of P-VB-NBu$_3$-Cl at a) 1M, b) 1.5 M and c) 2M concentrations of NaCl. Dashed line represents the transmittance curve of P-VB-NBu$_3$-Cl with appropriate concentration of NaCl as a function of temperature. For easier interpretation, every fifth point is shown on the graphs.

The use of $NaNO_3$ with aqueous solutions of P-VB-NBu$_3$-Cl results in a narrow range of clear transitions (Fig. 3.3.9). Thus, addition of NaCl to the system changed the nature of transitions from an irreversible in only $NaNO_3$ to a reversible in $NaNO_3$ and NaCl combination (Chapter 3.4). Although, in some concentrations addition of NaCl results in dissipation of a signal, wider range of LCST type phase separations can be observed in presence of both anions (Fig. 3.3.9 b). The solutions failing to provide a clear transition solely with NO_3^- anions (increasing the temperature results in formation of separate aggregates disrupting the outcome of the measurements), after introduction of NaCl show clear sharp transitions with a recognizable set of cloud point temperatures. This behavior might be a result of a "competition" between Cl^- and NO_3^- anions. Possibly, Cl^- binds to polymer much stronger than NO_3^-, resulting in higher demand of NO_3^- anions for the transition to occur (0.25 M NaCl is not enough for the solution with polymer to result in a transition Fig. 3.3.9 a.

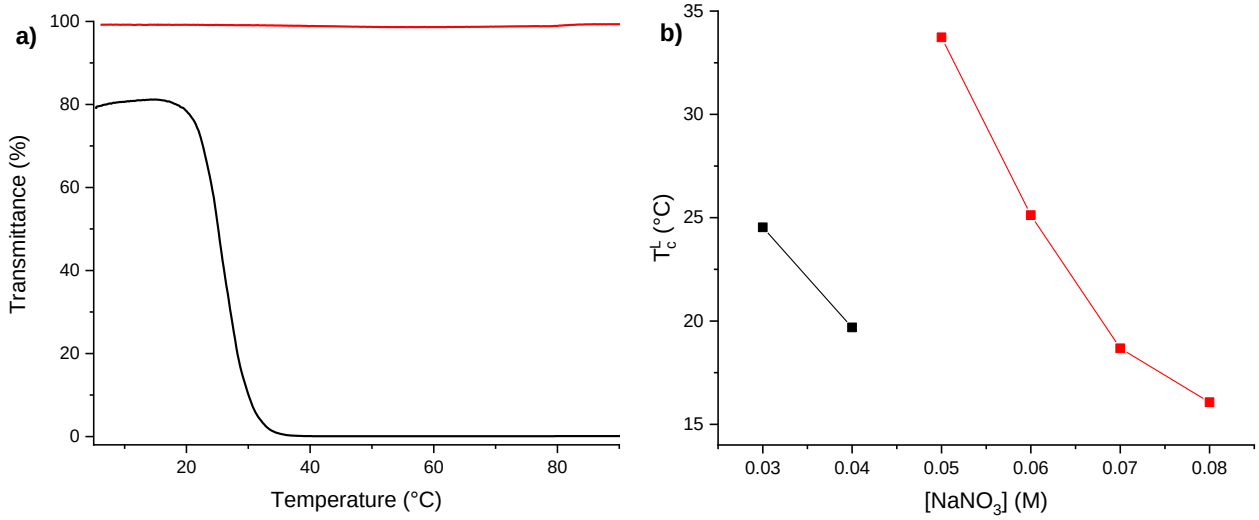

Fig. 3.3.9. a) Transmittance curves as function of temperature for 1 mg/ml water solutions of P-VB-NBu_3-Cl at concentrations of $NaNO_3$ of 0.025 M with (in red) and without (in black) NaCl (0.25 M). b) Dependence of the cloud point temperature on concentration of $NaNO_3$ in presence of 0.25 M NaCl (in red) and solely in $NaNO_3$ (in black).

It was difficult to determine the cloud point of the phase transition of P-VB-NBu_3-Cl and P-VB-$NPen_3$-Cl in presence of NaH_2PO_4. In H_2PO_4 anions system with P-VB-NBu_3-Cl (and P-VB-$NPen_3$-Cl) becomes viscous. Moreover, relatively higher concentrations are required for the turbidity to appear, no transition was observed for concentrations of NaH_2PO_4 below 2.7 M. The only reliable data was obtained from solutions taken to the analysis right after the sample preparation (Fig. 3.3.10). The behavior of polymer solutions with this particular anion needs more analysis.

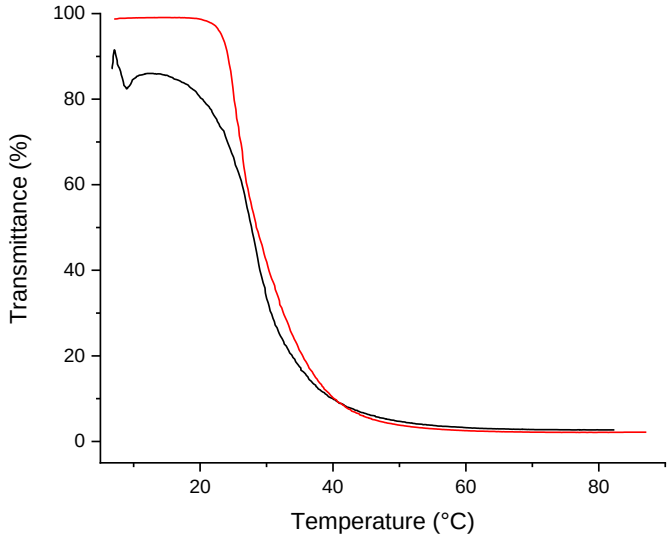

Fig. 3.3.10. Transmittance curves as function of temperature for P-VB-NBu_3-Cl in 3.2 M NaH_2PO_4 (black) and P-VB-$NPen_3$-Cl in 3.1 M NaH_2PO_4 (red)

3.3.4. P-VB-NPen$_3$-Cl

The behavior of P-VB-NPen$_3$-Cl with NaH_2PO_4 have already been discussed in section 3.3.3. and figure 3.3.10. In presence of NaCl aqueous solutions of P-VB-NPen$_3$-Cl express LCST type phase separation. P-VB-NPen$_3$-Cl is the only polymer from the VBA series to show a transition with Na_2SO_4 (Fig. 3.3.11. b). This kind of behavior towards the VBA series occurs due to low solubility of Na_2SO_4 in water at RT [86]. At 5°C ~1 M water solution of Na_2SO_4 precipitates to form transparent crystals.

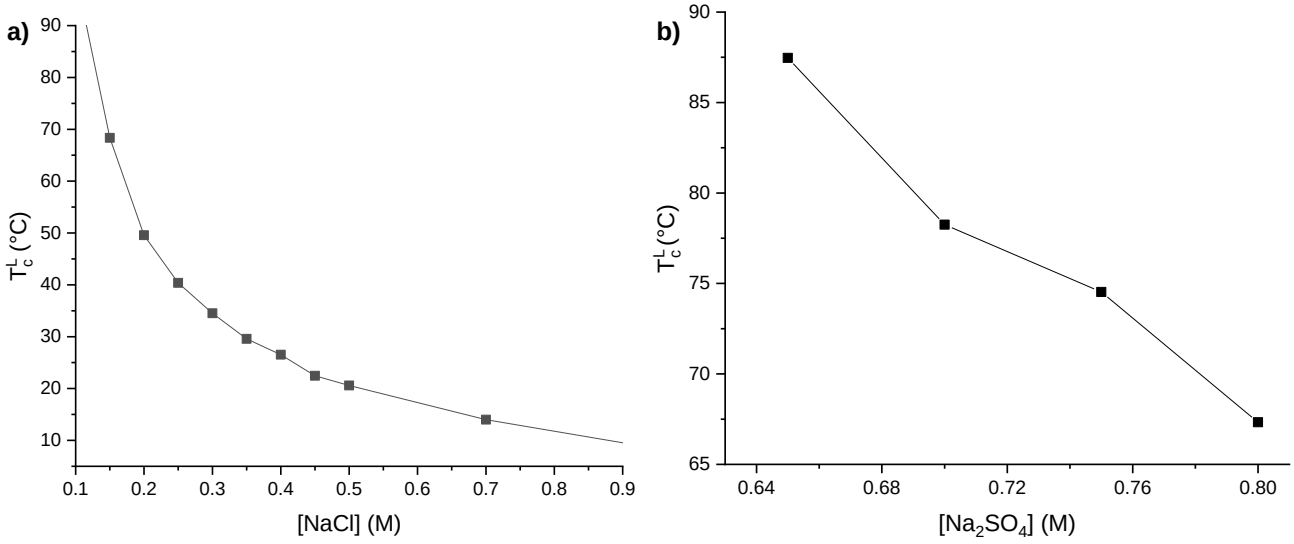

Fig. 3.3.11. Cloud point temperature curves for 1 mg/ml water solutions of P-VB-NPen$_3$-Cl as function of concentration of a) NaCl, b) Na_2SO_4.

In NaCl the system shows an exponential decrease of cloud point temperature depending on the concentration of anions (3.3.11 a), though much lower concentration of NaCl is needed for the first transition to occur. The behavior of P-VB-NPen$_3$-Cl in NaCl might help in understanding of the behavior of other polymers of VBA series with Na_2SO_4. Since P-VB-NBu$_3$-Cl solution demands higher concentrations of NaCl for the first transition than P-VB-NPen$_3$-Cl, it's only logical that P-VB-NBu$_3$-Cl demands higher concentrations of Na_2SO_4 (unachievable at RT) than P-VB-NPen$_3$-Cl. For better understanding of the aforementioned phenomenon, the following graph (Fig. 3.3.12) illustrates the NaCl concentration dependency of cloud point temperatures of P-VB-NPen$_3$-Cl, P-VB-NBu$_3$-Cl and P-VB-NPr$_3$-Cl.

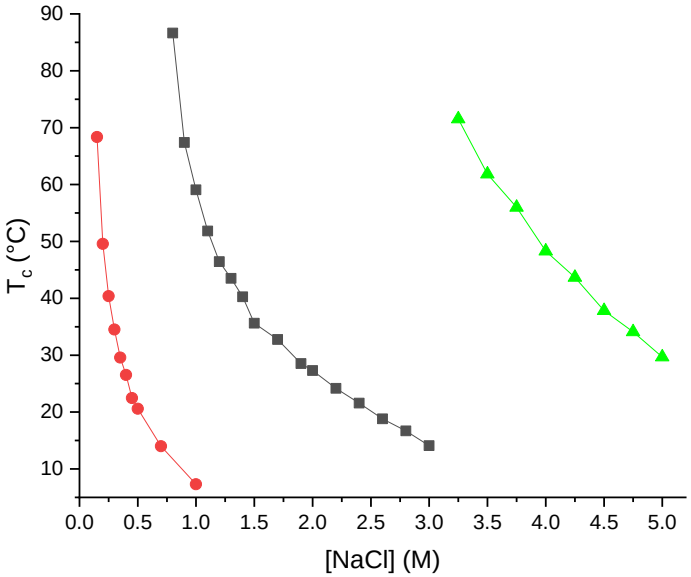

Fig. 3.3.12. Cloud point temperature curves for 1 mg/ml water solutions of P-VB-NPen$_3$-Cl (●), P-VB-NBu$_3$-Cl (■) and P-VB-NPr$_3$-Cl (▲) as function of concentration of NaCl.

Altogether, the phase transitions of Hofmeister series anions with VBA polymer series do not resemble any other types of transitions studied prior to this research [36, 37].

3.4. Reversibility

Thermoresponsive polymers usually show reversible phase transitions. For VBA polymer series number of anions from HS and counterions show irreversible transitions (Fig. 3.4.1.).

On one hand, none of the transitions demonstrate a completely reversible behavior with the same cloud point temperature. On the other hand, P-VB-NBu$_3$-Cl and P-VB-NPen$_3$-Cl show a reversible transition with NaCl with a slightly shifted cloud point temperature. PS anions show a reversible behavior with a shifted cloud point temperature as well. In these two cases T_c^L shifts to different directions. It's possible that the thermal history of the solution has a part in this behavior. When P-VB-NPr$_3$-Cl solutions combine with NaCl, the phase transition becomes only partially reversible. Keeping this sample at reduced temperatures does not affect the final transmittance of 40%.

Samples with nitrate and DS anions with P-VB-NBu$_3$-Cl also show an irreversible behavior. Even when the cooling starts right after the transition, the sample keeps turbidity at low temperature

regardless of time. The transition of P-VB-NPr_3-Cl with nitrate anions is partially reversible, allowing the observation of both LCST and UCST type phase transitons.

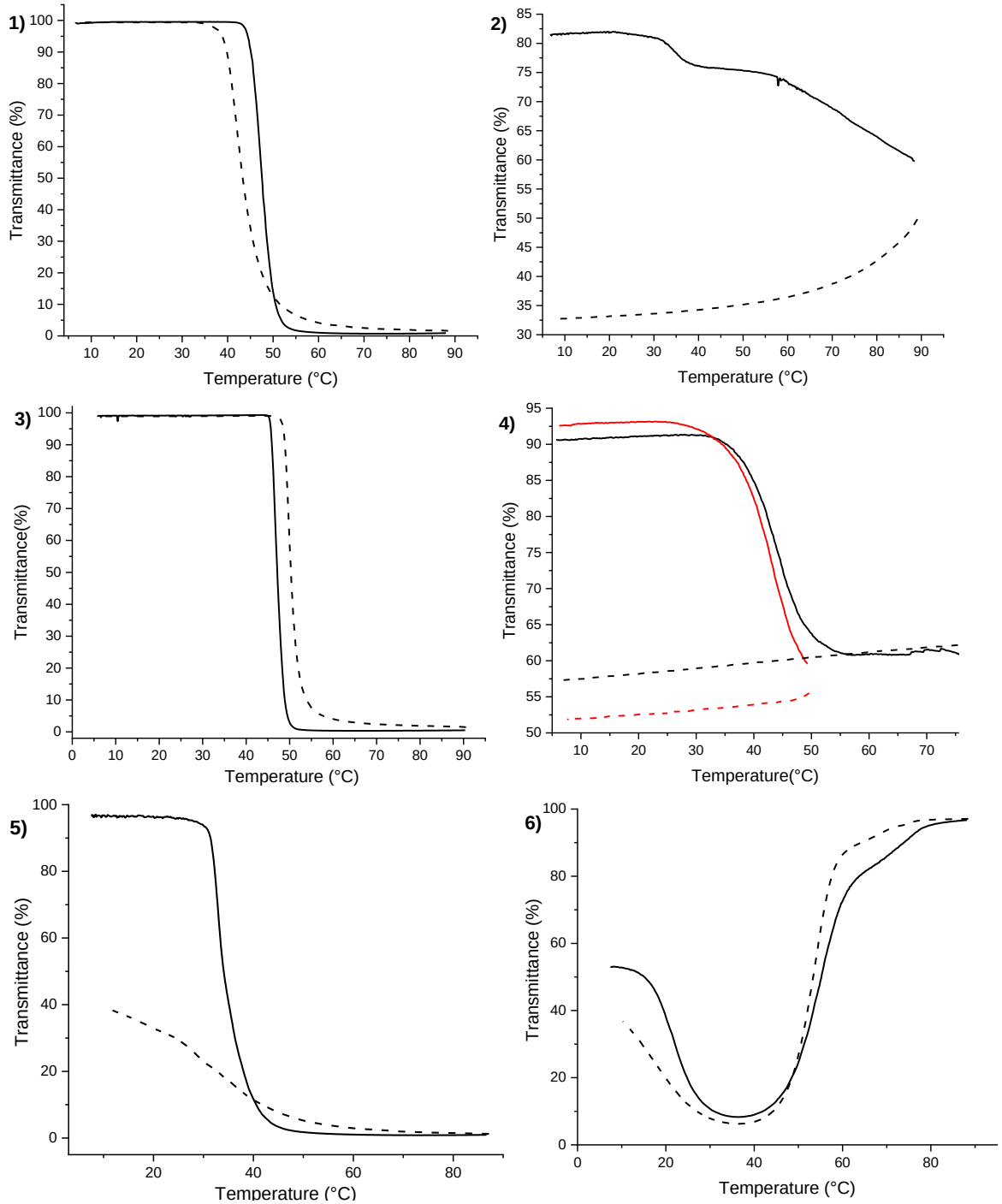

Fig. 3.4.1. The reversibility tests of VBA polymer series in presence of HS anions and counterions: 1) aqueous solutions of P-VB-NBu_3- Cl in presence of 1.2 M NaCl, 2) aqueous solutions of P-VB-NBu_3- Cl in presence of 0.2 M $NaNO_3$, 3) aqueous solutions of P-VB-NBu_3- Cl in presence of 0.1 M NaPS, 4) aqueous solutions of P-VB-NBu_3- Cl in presence of 0.3 mM SDS, 5) aqueous solutions of P-VB-NPr_3- Cl in presence of 5 M NaCl, 6) aqueous solutions of P-VB-NPr_3- Cl in presence of 200mM $NaNO_3$. Heating – solid lines, cooling – dashed lines. Black – temperature range between 5°C and 90°C, Red – temperature range between 5°C and 50°C.

3.5. Cononsolvency

Solution behavior of polymers from VBA series in different solvents was not a direct purpose of this research. Though, all the polymers including P-VB-$NHex_3$-Cl were perfectly soluble in methanol. Only P-VB-$NHex_3$-Cl, P-VB-NBu_3-Cl and P-VB-$NPen_3$-Cl were soluble in acetone, only P-VB-NEt_3-Cl was insoluble in DMF. The further investigations on solubility of these polymers in polar/non-polar solvents can give an important results to widen the knowledge about the solution behavior of the series.

The cononsolvency phenomenon was observed during dialysis of P-VB-NBu_3-Cl in water/DMF solution.

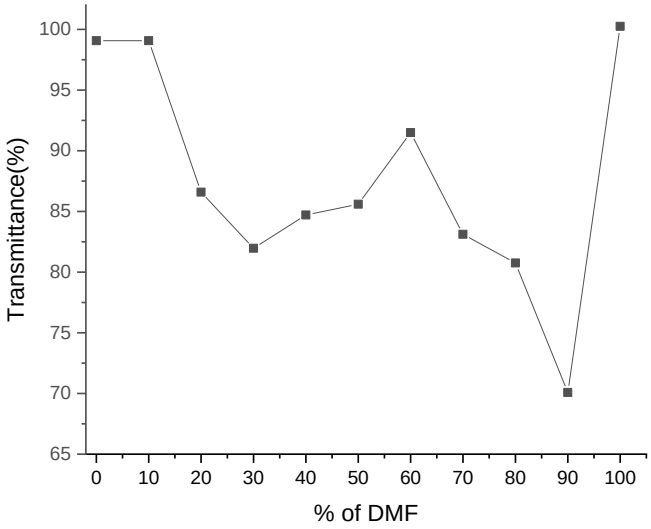

Fig. 3.5.1. Dependency of transmittance of aqueous solutions of P-VB-NBu_3-Cl on the percentage of added DMF

Neither heating, nor cooling of the turbid samples showed a phase transition. The turbidity only depends on the composition of solution. Non-linear dependency also states that this phenomenon occurs differently for P-VB-NBu_3-Cl than for commonly known LCST polymers as PNIPAm. Presence of charge can be a starting point to investigate the cononsolvency phenomenon in other solvents.

4. Conclusions

The research of the thermoresponsive properties of VBA polymer series resulted in discovery of two new LCST systems, a system with UCST and two systems with both LCST and UCST type phase transitions. Considering the fact that polymers differ only depending on the length of the alkyl tails of the quaternary ammonium, it's safe to assume, that this is the driving force of differences in the solution behavior of the new series of thermoresponsive polymers.

Many polycation-counterion demonstrate behavior never observed prior to this research. Surfactants as sodium dodecanesulfonate and sodium pentanesulfonate show an LCST type phase separation with P-VB-NBu_3-Cl and P-VB-$NPen_3$-Cl. The transitions, where the two-phased mixture is observed both before and after the cloud point temperature corresponds to only SDS surfactants. The author suggests, cooperative bonding takes place, resulting in micellar formation prior to the heating. LCST was observed only once with P-VB-NBu_3-Cl solutions in presence of PS counterions (and upon the addition of NaCl). P-VB-NEt_3-Cl shows either UCST or LCST type transitions depending on the counterions in the system.

Experiments with Hofmeister series show the fading of UCST type phase separation and prevalence of LCST type phase separation behavior upon increase of the length of alkyl tail of ammonium within the VBA polymer series.

Cononsolvency experiments indicate the presence of new type of phase separation independent of the temperature variation.

In future, more studies with other anions within HS may clarify the behavior of VBA polymer series. More particle size experiments might explain the particle formation with other counterions. The polymers can be used as films and hydrogels.

5. Appendixes

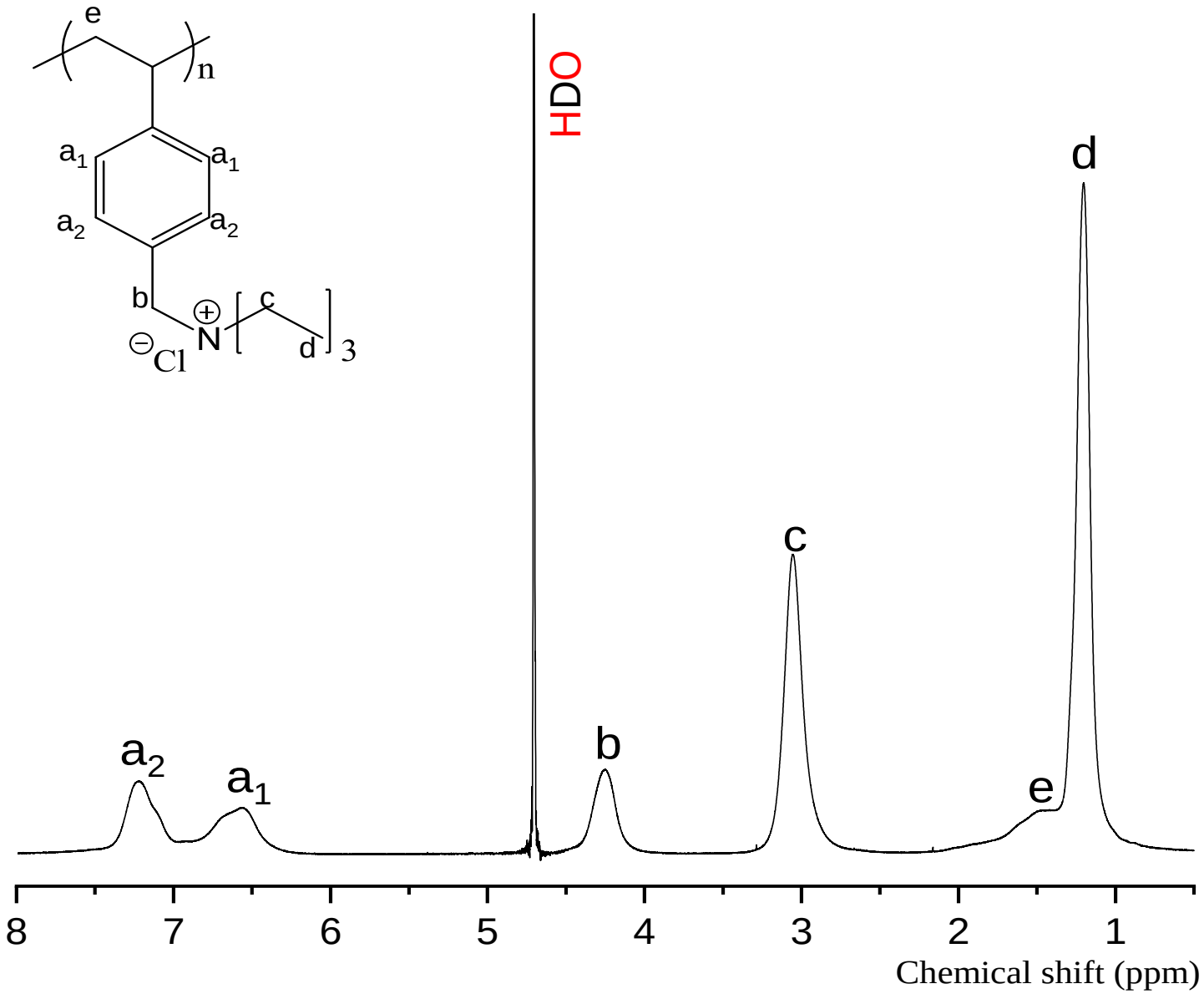

Appendix 1. ^{1}H NMR spectrum of Poly[(vinylbenzyl)triethyl]ammonium chloride in D_2O.

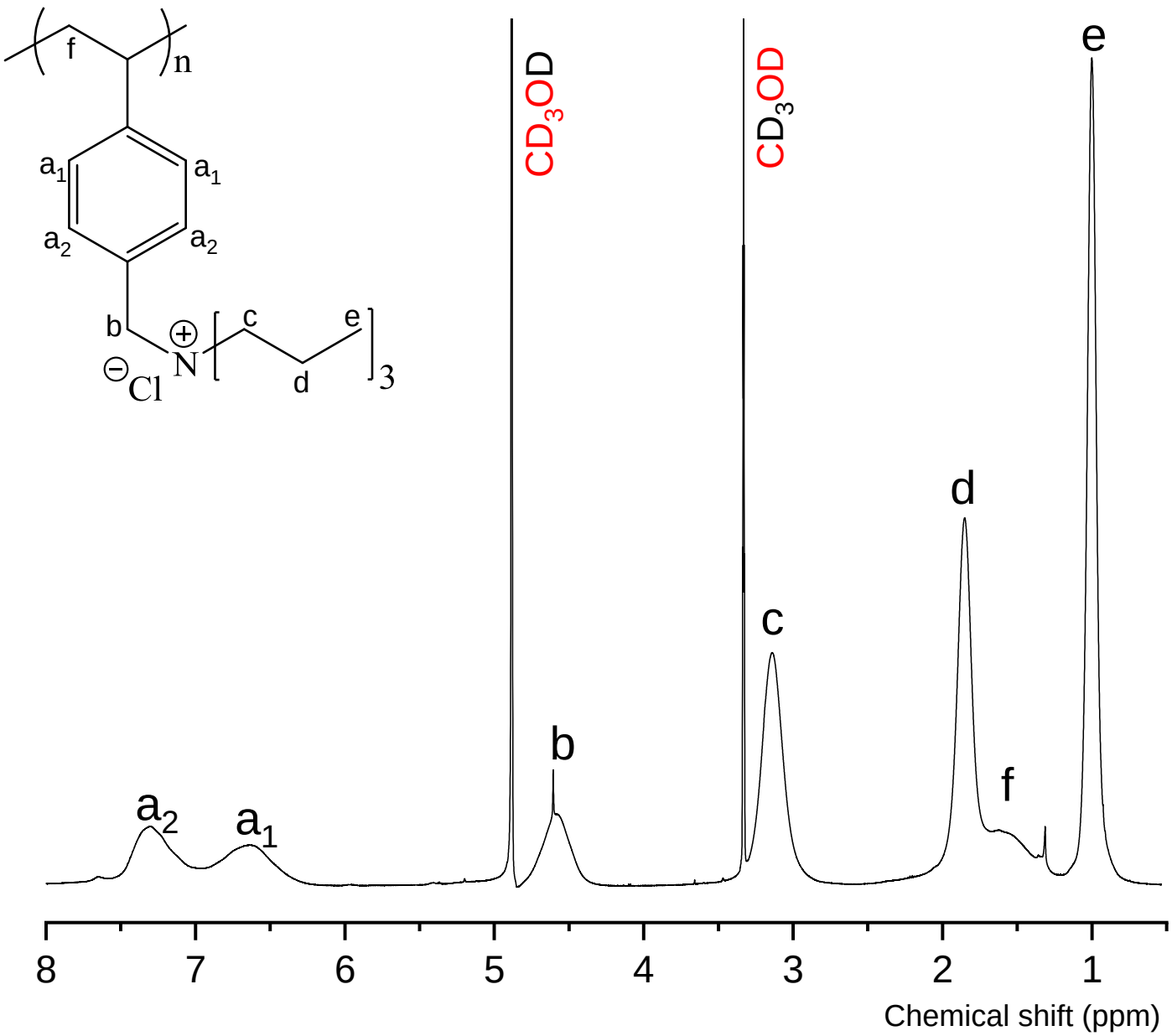

Appendix 2. ^{1}H NMR spectrum of Poly[(vinylbenzyl)tripropyl]ammonium chloride in MeOD.

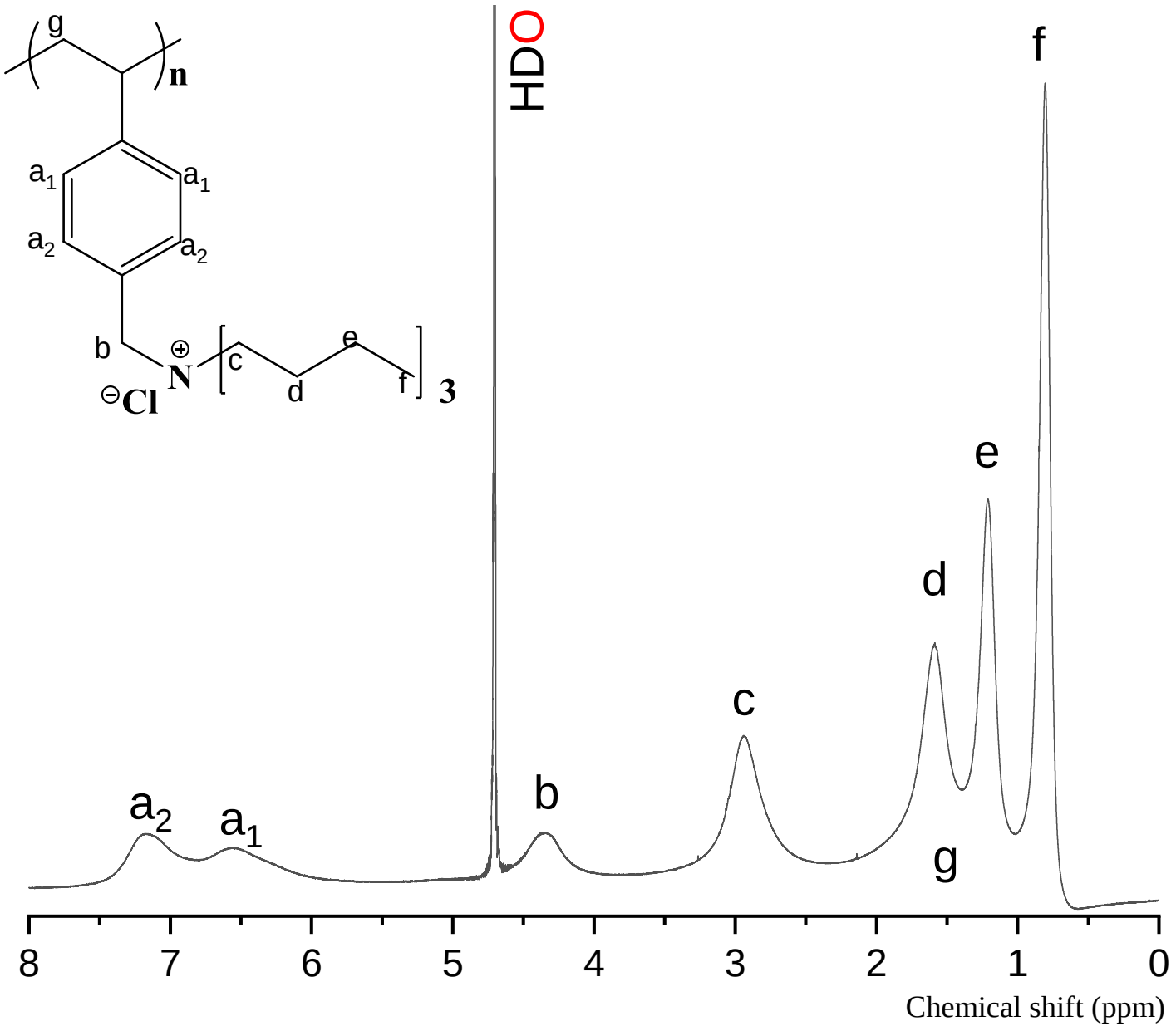

Appendix 3. ^{1}H NMR spectrum of Poly[(vinylbenzyl)tributyl]ammonium chloride in D_2O.

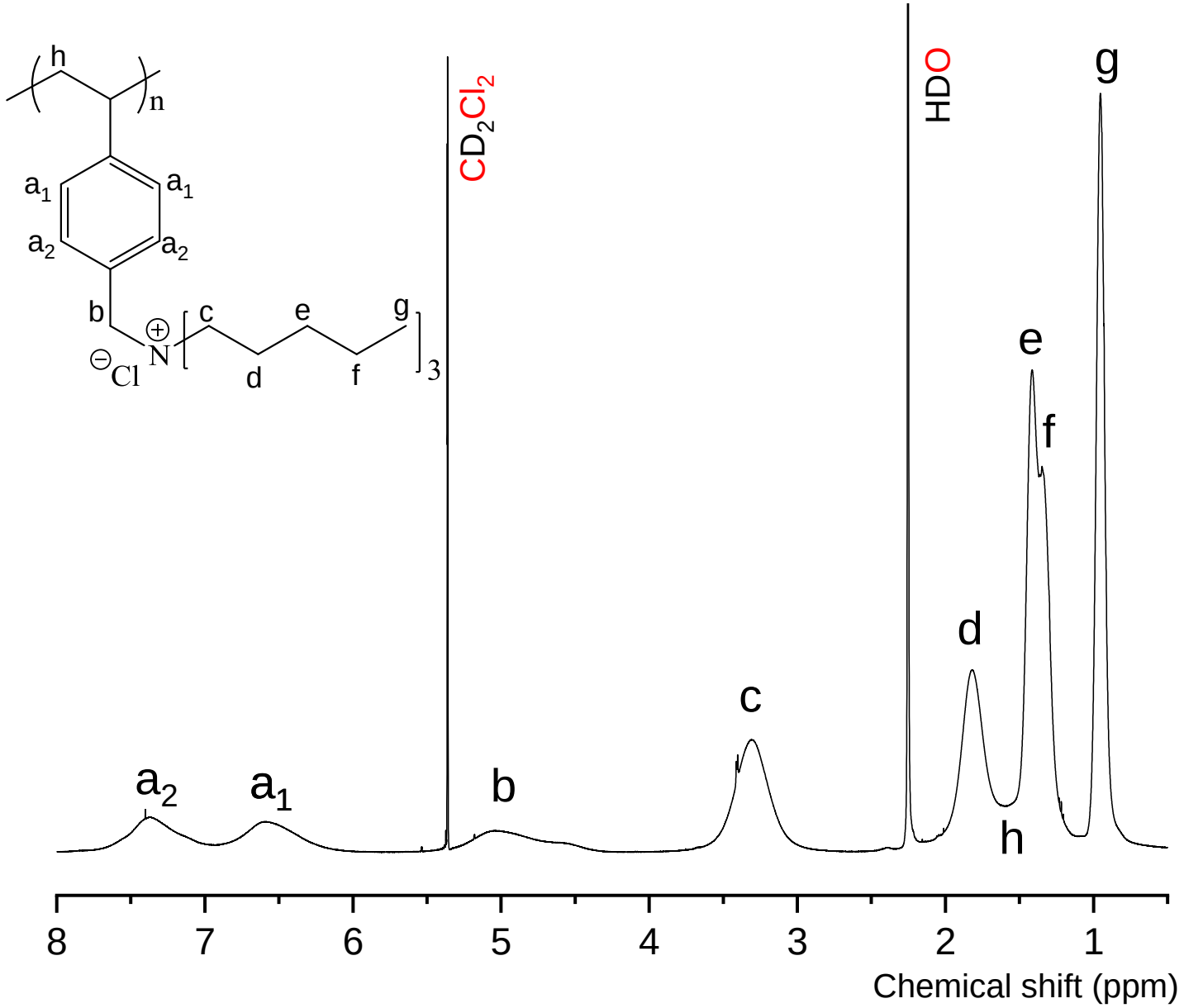

Appendix 4. ^{1}H NMR spectrum of Poly[(vinylbenzyl)tripentyl]ammonium chloride in CD_2Cl_2.

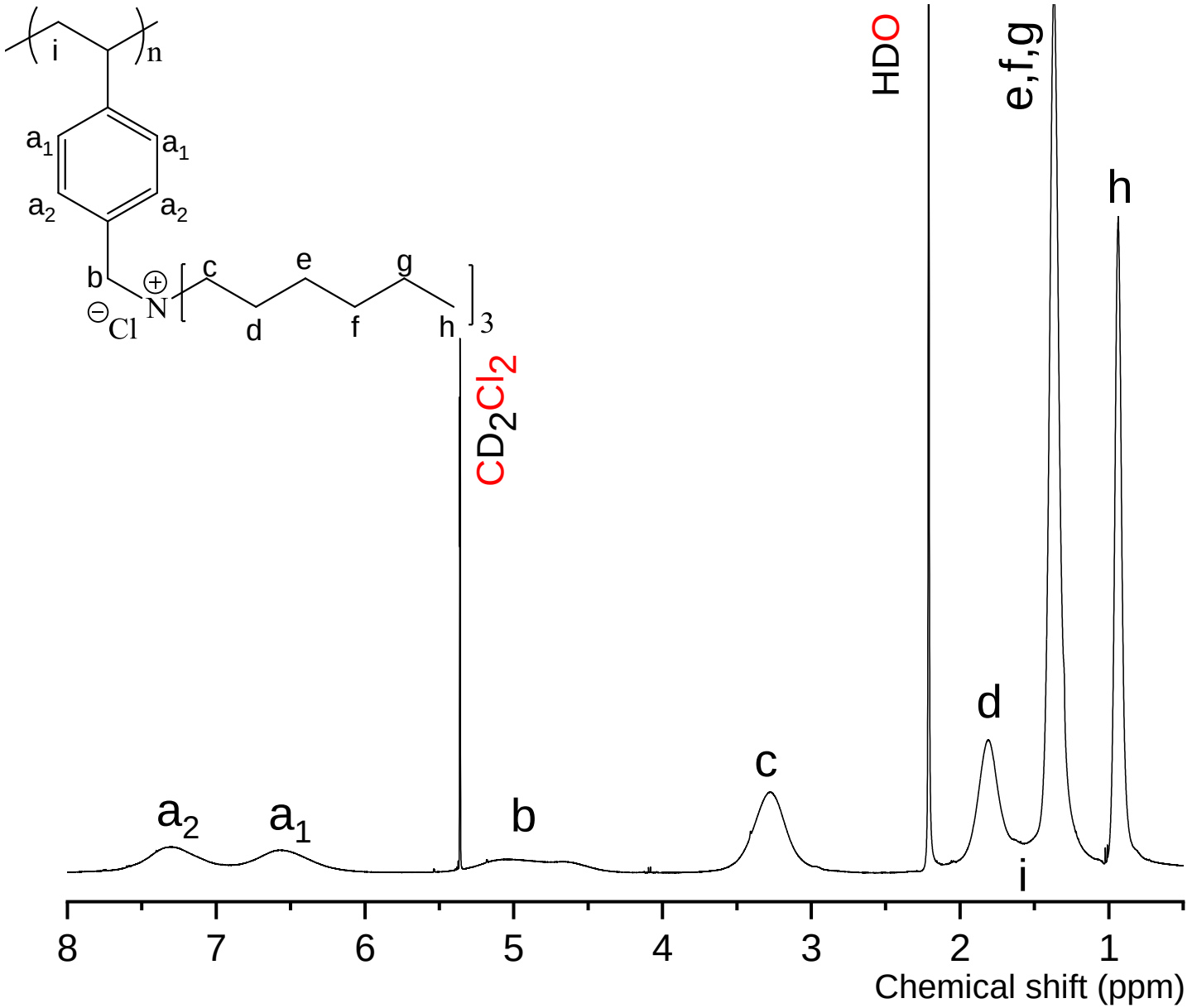

Appendix 5. ^{1}H NMR spectrum of Poly[(vinylbenzyl)trihexyl]ammonium chloride in CD_2Cl_2.

6. References

1. Wei, M.; Gao, Y.; Li, Xue.; Serpe, M. *J. Polym. Chem.* 2017, 8, 127–143
2. Zhang, Q.; Weber, C.; Schubert, U. S.; Hoogenboom, R. *Roy. Soc. Chem*, Mater. Horiz., 2017, 4, 109—116
3. Shimada, N.; Maruyama, A. *Tail. Polym. Arch. Phar m. Biomed. Appl.* 2013, 14, 235-241
4. Mohammed, M. N.; Bin Yusoh, K.; Binti Haji, S.; Jun, H. *Mat. Exp.*, 2018, 8, 1, 21-34
5. Weiss, T.; Seelmann-Eggebert, HP.; Weidl, C. H.; Raether, R. B. *BASF SE.*
6. Fu, W.; Bai, W.; Jiang, S.; Seymour, B.; Zhao, B.; *Macromol.*, 2018, 51, 5, 1674-1680
7. Thakur, N.; Baji, A.; Ranganath, A.S. *Appl. Surf. Sci.*, 2018, 433, 1018-1024
8. Zhu, Y.; Batchelor, R.; Lowe, A.B.; Roth, P.J. *Macromol.* 2016, 49, 672−680
9. Lin, S.; Schattling, P.; Theato, *P. Sci. Adv. Mater.* 2015, 7, 948−955.
10. Gohy, J.-F.; Zhao, Y. *Chem. Soc. Rev.* 2013, 42, 7117−7129.
11. Jochum, F. D.; Theato, P. *Chem. Soc. Rev.* 2013, 42, 7468−7483.
12. Phillips, D. J.; Gibson, M. I. *Antioxid. Redox Sign.* 2014, 21,786−803.
13. Aseyev, V. O.; Tenhu, H.; Winnik, F. M. *Adv. Polym. Sci*. 2011, 242, 29–89
14. Schild, H. G. *Progress in Polymer Science*, 1992, 17 (2), 163–249.
15. Heskins, M.; Guillet, J. E. *J. Macromol. Sci.* 1968, 2, 1441-1455
16. Men, Y.; Schlaad, H.; Yuan, J.; *ACS Macro Lett.* 2013, 2, 456-459
17. Inoue, K.; Aikawa, S.; Fukushima, Y. *Polym. Int.* 2018, 67, 6, 755-760
18. Chytrý, V.; Ulbrich, K. *J. Bioact. Compat. Polym.* 2001, 16, 427
19. Bou, S. J. M. C.; Connolly, A. R.; Ellis, A. V. *Roy. Soc. Chem.*, 2018
20. Chakraborty, I.; Mukherjee, K.; De, P.; Bhattacharyya, R. *J. Phys. Chem. B* 2018, 122, 6094 - 6100
21. Aseyev, V. O.; Tenhu, H.; Winnik, F. M. *Adv. Polym. Sci*. 2006, 196, 1-85

22. Meeussen, F.; Nies, E.; Berghmans, H.; Verbrugghe, S.; Goethals, E.; Du Prez, F. *Polymer* 2000 41:8597

23. Afroze, F.; Nies, E.; Berghmans, H. *J. Mol. Struct.* 2000, 554, 55

24. Schäfer-Soenen, H.; Moerkerke, R.; Berghmans, H.; Koningsveld, R.; Dušek, K.; Solc, K. *Macromolecules* 1997, 30, 410–416.

25. Swier, S.; Van Durme, K.; Van Mele, B. J. Polym. Sci. Polym. Phys. 2003, 41, 1824

26. Nayak, P. K.; Hathorneb A. P.; Bermudez, H. *RSC Pub.* 2013

27. Costa, M. C. M.; Silva, S. M. C.; Antunes, F. E.; *J. Mol. Liq.* 2015, 210, A, 113-118

28. Ueki, T.; Watanabe, M. *Langmuir*, 2007, 23, 988–990.

29. Elaissaf, J.; *J. Appl. Polym. Sci.* 22, 873 (1978).

30. Schild, H. G.; Tirell, D. A. *Polym. Prepr*. 1989 30(2), 350

31. Schild, H. G.; Tirell, D. A. *Langmuir* 7, 665 (1991).

32. Schild, H. G. *ACS Syrup. SeE*. 467, Chap. 17 (1991).

33. Racka, J.; Mewes, M.; Nyrfregger; Bernardt, *T. Phys. Rev. Lett*. 65, 657 (1990).

34. Schild, H. G.; Tirell, D. A., *J. Phys. Chem.* 94, 4352 (1990).

35. Zhang, J.; Cremer, P.S. *Cur. Op. in Chem. Bio.* 2006, 10, 658-663

36. Zhang, J.; Furyk, S.; Bergbreiter, D. E.; Cremer, P.S. *J. of Am. Chem. Soc.* 2005, 127, 41, 14505-14510

37. Heyda, J.; Dzubiella, J.; *J. of Phys. Chem. B* 2014, 118, 37, 10979-10988

38. Karjalainen, E.; Aseyev, V.; Tenhu, H. *Polym. Chem.* 2015, 6, 16, 3074-3082

39. Tanaka F., Koga T., Winnik F., *Progr. Colloid Polym. Sci.* 2009, 136, 1–8

40. Tanaka F., Koga T., Kojima H., Xue N., Winnik F.M., *Macromol.* 2011, 44, 2978–2989

41. Zhang, G.; Wu, C. *J. Am. Chem. Soc.* 2001, 123, 137

42. Hao, J.; Cheng, H.; Butler, P.; Zhang, L.; Han, C. C. *J. Chem. Phys.* 2010, 132, 154902[1-9].

43. Gandhi, A.; Paul, A.; Sen, S. O.; Sen, K. K. *As. J. Pharm. Sci.* 2915, 99–107

44. Idziak, I.; Avoce, D.; Lessard, D.; Gravel, D.; Zhu, X. X. *Macromolecules* 1999, *32*, 1260–1263

45. Moerkerke, R.; Meeussen, F.; Koningsveld, R. *et al. Macromolecules* 1998, 31, 2223-2229

46. Van Durme, K.; Mele, B. V.; Bernaerts, K. V.; Verdonck, B.; Prez, F. E.; *J. Polym. Sci. P. B: Polym. Phys.* 2006, 44, 2, 461-469, 1099-0488

47. Solomon, O. F.; Corciovei, M.; Ciuta, I.; Boghina, C. *J. Appl. Polym. Sci.* 1968; 12:1835–42.

48. Cortez-Lemus, N. A.; Licea-Claverie, A. *Progr. Polym. Sci.* 2016, 53 1–51

49. Etchenausia, L.; Deniau, E.; Brulet, A.; Forcada, J.; Save, M. *Macromolecules* 2018, 51, 2551−2563

50. Seuring, J.; Agarwal, S. *Macromol. Rapid Commun.* 2012, *33*, 1898−1920

51. Seuring, J.; Agarwal, S. *ACS Macro Lett*. 2013, 2, 597-600.

52. Zheng, L.; Sundaram, H. S.; Wei, Z.; Li, C.; Yuan, Z.; *Reac. Fun. Polym.* 2017, 118, 51–61

53. Haas, H. C.; Schuler, N. W. *Polym. Lett.* 1964, *2*, 1095

54. Seuring, J.; Bayer, F.M.; Huber, K.; Agarwal, S.; *Macromolecules* 2012, 45, 374-384

55. Oosawa, F. *Marcel Dekker, Inc.*, New York 1971, 1-12

56. Plamper, F. A.; Schmalz, A.; Ballauff, M.; Müller, A. H. E.; *J. Am. Chem. Soc.*, 2007, 129, 14538–14539

57. Plamper, F. A.; Ruppel, M.; Schmalz, A.; Borisov, O.; Ballauff, M.; Müller, A. H. E.; *Macromolecules* 2007, 40,8361–8366

58. Liu, Q.; Yu, Z.; Ni, P. *Colloid Polym. Sci.* 2004, *282*, 387–393.

59. Burillo, G.; Bucio, E.; Arenas, E.; Lopez, G. P. *Macromol. Mater. Eng.* 2007, *292*, 214–219.

60. Karjalainen, E.; Aseyev, V.; Tenhu, H. *Macromolecules* 2014, 47, 2103-2111

61. Schmalz, A.; Hanissch, M.; Schmalz, H.; Müller A. H. E. *Polymer* 2010, 51, 6, 1213-1217

62. Bütün, V.; Armes, S. P.; Bilingham, N. C. *Polymer* 2001, 42, 14, 5993-6008

63. Chen, C-Y.; Wang, H-L. *Macromol. Rapid Commun.* 2014, 35, 17, 1534-1540

64. Thavanesan, T.; Herbert, C.; Plamper, F. A. *Langmuir* 2014, 30, 5609-5619

65. Men, Y.; Schlaad, H.; Yuan, J. *ACS Macro Lett.* 2013**,** *2*, 456–459

66. Kohno, Y.; Deguchi, Y.; Inoue, N.; Ohno, H. *Aust. J. Chem.* 2013**,** *66*, 1393–1398.

67. Karjalainen, E.; Aseyev, V.; Tenhu, H. *Macromolecules* 2014, 47, 7581–7587

68. Matyjaszewski, K.; Spanswick, J. *MaterialsToday* 2005, 8, 3, 26-33

69. Mishra. V.; Kumar, R. *J. of Sci. Res.* 2012, 56, 141–176

70. Hawker, C. J.; Bosman, A. W.; Harth, E. *Chem. Rev.* 2001, 101 (12), 3661–3688

71. Perrier, S. *Macromol.* 2017, 50, 7433-7447

72. Moad, G.; Rizzardo, E.; Thang, S. H. *Polymer* 2008, 49, 5, 1079-1131

73. García-Lopera, R.; Codoñer, A.; Baño, M. C.; Abad, C.; Campos, *A. J. Chrom. Sci.* 2005, 43

74. D'Agosto, F.; Hughes, R.; Charreyre, M. T., Pichot, C.; Gilbert, R. G. *Macromolecules* 2003, 36, 621-629

75. Kohno, Y.; Deguchi, Y.; Inoue, N.; Ohno, H. *Aust. J. Chem.* 2013**,** *66*, 1393–1398.

76. Xue, L.; Padgett, W. C.; DesMarteau, D. D.; Pennington, W. T. *Sol. State Sci.* 2002, 4, 11-12, 1535-1545

77. Sano, T.; Nakatsuka, T.; Tsuruta, H.; Harada, S. *Bull. Chem. Soc. Jpn*. 1987, 60, 759–760

78. Schwarz, G. *Eur. J. Biochem.* 1970, 12, 442 – 453

79. Okuzaki, H.; Osada, Y.; *Macromolecules* 1994, 27, 502–506

80. Zhu, P. W.; Napper, D. H. *Langmuir* 1996**,** *12*, 5992–5998

81. Yaminsky, V. V.; Vogler, E. A. *Cur. Op. Col. Int. Sci.* 2001, 6, 4, 342 – 349

82. Wang, X.; Qui, X.; Wu, C. *Macromolecules* 1998, 31, 2972 – 2976

83. Burgess, J. *Metal Ions in Solution* 1978

84. Van Durme, K.; Van Assche, G.; Van Mele, B. *Macromolecules* 2004, 37, 9596 – 9605

85. Burba, C. M.; Carter, S. M.; Mayer, K. J.; Rice, C. V. *J. Phys. Chem. B* 2008, 112, 10399-10404

86. Okorafor, C.O. *J. Chem. Eng. Data* 1999**,** *44*, 488–490